Meteor Berichte 05

Mid-Atlantic Expedition 2005

Cruise No. 64, Leg 1

MARSÜD 2

2 April – 3 May 2005, Mindelo (Cape Verde) – Fortaleza (Brazil)

K. Haase, C. Flies, S. Fretzdorff, O.Giere, A. Houk, S. Klar, A. Koschinsky, J. Küver, H. Marbler, P. Mason, N. Nowald, C. Ostertag-Henning, H. Paulick, M. Perner, S. Petersen, V. Ratmeyer,W. Schmidt, T. Schott, M. Schröder, R. Seifert, C. Seiter, J. Stecher, H. Strauss, J. Süling, D. Unverricht, M. Warmuth, S. Weber, U. Westernströer

Project Leader: Karsten Haase

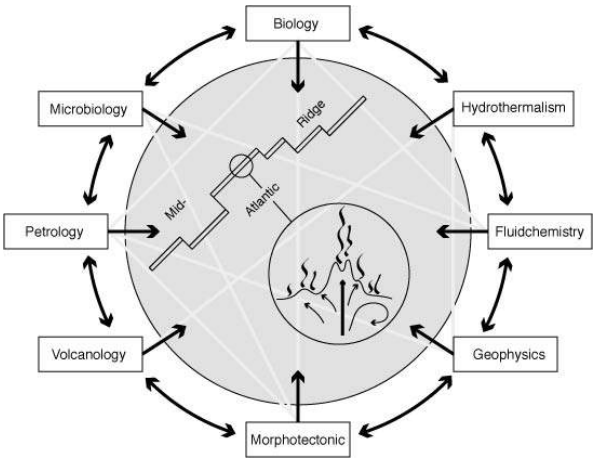

Leitstelle Meteor
Institut für Meereskunde der Universität Hamburg

2005

1. Leg M64/1

1.1. Participants

PD Dr. Karsten Haase, chief scientist	IfG Uni Kiel
Dr. Christine Flies	GZ Göttingen
Dr. Susanne Fretzdorff	IfG Uni Kiel
Prof. Dr. Olav Giere	ZIM Hamburg
Andy Houk	Schilling Robotics, Davis
Steffen Klar	MARUM Bremen
PD Dr. Andrea Koschinsky	IU Bremen
Dr. Jan Küver	MPA Bremen
Dr. Herwig Marbler	IU Bremen
Pete Mason	SOC Southampton
Nicolas Nowald	MARUM Bremen
Dr. Christian Ostertag-Henning	BGR Hannover
Dr. Holger Paulick	MinBonn
Mirjam Perner	IfM-Geomar Kiel§
Dr. Sven Petersen	IfM-Geomar Kiel#
Dr. Volker Ratmeyer	MARUM Bremen
Werner Schmidt	MARUM Bremen
Thorsten Schott	IfM-Geomar Kiel#
Marcel Schröder	MARUM Bremen
Dr. Richard Seifert	IFBM Hamburg
Christian Seiter	MARUM Bremen
Dr. Jens Stecher	FSI Wilhelmshaven
Prof. Dr. Harald Strauss	GPI Münster
Dr. Jörg Süling	IfM-Geomar Kiel§
Daniel Unverricht	IfG Kiel
Marco Warmuth	IFBM Hamburg
Stefan Weber	IFBM Hamburg
Ulrike Westernströer	IfG Kiel

Abbreviations:

BGR Hannover: Bundesanstalt für Geowissenschaften und Rohstoffe, Stilleweg 2, D-30655 Hannover

FSI Wilhelmshaven: Forschungsinstitut Senckenberg, Rheinstrasse 190, D-26382 Wilhelmshaven, Germany

GPI Münster: Geologisch-Paläontologisches Institut, Corrensstraße 24, D-48149 Münster, Germany

GZG: Göttinger Zentrum Geowissenschaften GZG, Abt. Geobiologie, Universität Göttingen, Goldschmidtstr. 3, D-37077 Göttingen, Germany

IFBM Hamburg: Institut für Biogeochemie und Meereschemie, Bundesstr. 55, D-20146 Hamburg, Germany

IfG Uni Kiel : Institut für Geowissenschaften, Abteilung Geologie, Christian-Albrechts-Universität zu Kiel, Olshausenstr. 40, D-24118 Kiel, Germany

IfM-Geomar Kiel§: Leibniz-Institut für Meereswissenschaften, IFM-GEOMAR, Düsternbrooker Weg 20, D-24105 Kiel, Germany

IfM-Geomar Kiel#: Leibniz-Institut für Meereswissenschaften, IFM-GEOMAR, Dienstgebäude Ostufer, Wischhofstr. 1-3, D-24148 Kiel, Germany

IU Bremen: Geosciences and Astrophysics, Research III, Room 108, School of Engineering and Science, International University Bremen IUB, Campus Ring 8, D-28759 Bremen, Germany

MARUM Bremen: MARUM Zentrum für Marine Umweltwissenschaften, Universität Bremen, Leobener Str, D-28359 Bremen, Germany

MinBonn: Mineralogisches und Petrologisches Institut, Universität Bonn, Poppelsdorfer Schloss, D-53115 Bonn, Germany

MPA Bremen: Department of Microbiology, Bremen Institute for Materials Testing, a Division of the Institute for Materials Science, Paul-Feller-Str. 1, D-28199 Bremen, Germany.

SOC Southampton: Southampton Oceanography Centre, European Way, Empress Dock, Southampton SO14 3ZH, United Kingdom

ZIM Hamburg:

Zoologisches Institut und Zoologisches Museum, Universität Hamburg, Martin-Luther-King-Platz 3, D-20146 Hamburg, Germany

1.2. Research Program

Mid-ocean ridges are unique features of the Earth where energy and material is exchanged between the Earth's interior and the surface. This cruise is part of a DFG Priority Programme "From Mantle to Ocean: Energy, material and life cycles on spreading axes" designed to obtain a four-dimensional picture of the processes operating at mid-ocean ridges. In this context the overall goals of the planned investigations are as follows: (1) to determine the volcanic and tectonic dynamics operating at mid-ocean ridges as well as the geochemical and biological processes occurring at active hydrothermal vent areas shall be characterised in detail as a function of space and time and (2) to link the hydrothermal processes to the volcanic activity on the axis. The target area of Leg 64/1 is one of the two key areas of the Priority Programme 1144 on the Mid-Atlantic-Ridge (MAR) planned to be investigated by petrologists, biologists, chemists, geochemists, geophysists and oceanographers. It is situated between 7 and 12°S along the MAR south of the Ascension fracture zone (Figure M64/1-1). This section of the MAR is highly variable in morphology, crustal thickness, and magma composition and is thus an ideal region to study the diversity of magma transport and volcanic eruption processes and their influence on the formation and evolution of hydrothermal vents and associated biological processes. Leg M64/1 is a follow-up cruise of Leg M62/5 during which the foundation for this cruise – a detailed geologic and tectonic map of the seafloor and the position of hydrothermal plumes – has been obtained by using a TOBI combination of deep towed sidescan and nephelometry and a Remotely Operated Vehicle (ROV) and a CTD/Rosette. Based on this data our research group will select hydrothermally active sites and characterise them volcanologically, geochemically and biologically by taking and analysing rock samples, samples of hydrothermal fluids, samples of the micro- and macro fauna and samples of the water column in the vicinity of those vent areas.

1.3. Narrative of the cruise

The cruise started in Mindelo with some minor problems with the transport of crew members and with the successful loading of the heavy ROV containers with an ancient swimming crane. In the morning of April 2nd FS METEOR left the port of Mindelo and steamed southwards to the first working area on the Mid-Atlantic Ridge near 5°S. Throughout the cruise we had warm and calm weather and only for a couple of days the wind rose to a strength of 6 and the swell increased to about 3 m. In the evening of April 7th we arrived in the first working area at the location of the Turtle Pits hydrothermal field which was discovered only weeks before by a British-American cruise and the location of which was kindly forwarded to us by C. German and T. Shank. During the night the area was mapped with Hydrosweep after we had one CTD/rosette station outside of the ridge area in order to determine the background water composition. Unfortunately, the CTD failed and no water samples were recovered. On the morning of April 8th we performed the first dive (#36, station 108) with the MARUM QUEST ROV and after a few technical problems the ROV reached the seafloor at around noon. Towards the end of the dive we found two inactive balck smokers and deployed a sonar buoy. During the night two TV grab and several wax corer stations recovered basaltic lava and CTD/rosette stations were carried out to determine the location of the hydrothermal plume. MAPRs were also deployed with each wax corer and TV grab in order to study the areal extent of the plume. On April 9th the second ROV (#37, station

114) dive found the active chimneys situated in a north-south running depression and we started photographing, sampling and measuring the different structures. Between April 9th and April 15th five dives with the ROV were performed mostly during the day with CTD, wax corer and TV grab stations during the night. In most dives we studied the Turtle Pits field but one dive (#39, station 125) led to the Wideawake mussel field for geological, biological and fluid sampling. On April 16th a very long dive (#42, station 146) was performed starting south of the Turtle Pits field and ending at the Red Lion hydrothermal field where one active smoker had been reported by our British-American colleagues. While diving at this location we found four active smokers and numerous inactive structures with a peculiar fauna consisting of impressive numbers of shrimps. After this long dive we had a 24 h transit to the working area at 8°50´S on the MAR.

Work in this area started with a detailed bathymetric survey of the large volcanic field on segment A2. After that the lavas of the volcanic field were sampled using the wax corer and the ROV during two dives in order to study the volcanology and geology of the area. Surprisingly, much of the volcanic field was covered by sediments althought the sidescan maps showed a very high reflectivity. CTD and MAPR stations in the area of the volcanic field did not show any hydrothermal signal and we concluded that the southern part of segment A2 is probably both volcanically and hydrothermally inactive. After three days of work on segment A2 (April 18th to 21st) we continued hydrothermal exploration on segment A3 using wax corers with MAPRs and CTD/rosettes. 186 CTD station showed a strong methane anomaly but the nephelometers did not record any anomalies in the water column. On April 23rd and 24th we performed two dives on the shallowest part of segment A3 near the near-axis seamounts in order to study the volcanology and sample lavas. On the night from April 24th to the 25th five CTD stations defined the location of a potential hydrothermal vent to be within the area between 9°32.5´S and 9°33.0´S. Studying the bathymetric and sidescan maps indicated that the most likely location of a vent would be the neovolcanic zone with a narrow cleft. On the morning of the 25th the ROV dive led us from one of the CTD stations with an anomaly to the east toward the neovolcanic zone. At about 12 o´clock we found the first hydrothermal sediments and mussel shells and at 15:55 we discovered the active low-temperature Lilliput hydrothermal field. The name was given because of the overabundance of small baby mussels. Biological, geological and fluid samples were taken. During the night two TV grab stations recovered more hydrothermal sediment, lava and biology from this field. On the next morning the ROV started the dive but technical problems required to retrieve the ROV after 2 hours from the water. The final stations of cruise M64/1 consisted of CTD, wax corer, and TV grab stations and one camera sledge tow across the neovolcanic zone. On the 27th at 15:00 we finished our work and RV METEOR started its voyage to Fortaleza. The ROV team was busy repairing the damage in the high voltage unit of the ROV and was successful so that by the time of arrival in Fortaleza most of the damage was repaired. Early in the morning on May 3rd METEOR arrived in Fortaleza after a very successful cruise.

1.4. Preliminary Results

1.4.1. Geology and petrology

1.4.1.1. Geological setting and lava petrology of the area at 4°48`S on the MAR

(K. Haase, S. Fretzdorff, H. Paulick, D. Unverricht)

The Turtle Pits hydrothermal field occurs in a N-S striking row of collapse pits in a large sheet flow whereas the Wideawake Mussel Field occurs in a jumbled sheet flow. The abundance of fresh glassy sheet flows in the area suggests a very strong volcanic activity and the youngest observed lava covers parts of the Wideawake Mussel Field in the SE and is thus probably less than 10 years old. The segment was seismically active in June 2002 (C. Devey, pers. comm.) and one can speculate whether the seismic acitvity occurred during the eruption of the lava flow. These observations indicate that this segment of the MAR is currently in a volcanic rather than in a tectonic phase. The tectonic features of the MAR at 4°48´S all strike in N-S direction, for example, the major faults at the rift flanks, minor faults observed during ROV dives as well as volcanic features in the rift. Interestingly, the shallow rift flanks of the MAR at 4°48´S suggest variable volumes of magma production.

The volcanic rocks in the region surrounding the Turtle Pits hydrothermal and Wideawake Mussel fields have been sampled very detailed using the rock corer, TV grab and the ROV. Fourtytwo samples have been selected from the recovered lavas covering an area of about 3 x 3 km^2. Most of the lavas in this region are very fresh aphyric sheet flows with ropy and jumbled surfaces. Collapse structures with lava pillars are frequent in the sheet flows. Young lava flows also occur in the deep basin between the Turtle Pits hydrothermal field and the axial seamount (e.g. sample 146ROV-2). The freshness and the predominance of sheet flows in the region implies very strong volcanic activity and eruption volumes in this segment of the Mid-Atlantic Ridge. Pillow lavas occur only in few areas, for example, on the small seamount west of the Turtle Pits field and on the very young lavas in the south of the Wideawake Mussel field.

Most lavas are glassy and aphyric without vesicles suggesting that the magmas were undersaturated with volatiles either due to the high water pressure or low volatile concentrations. From the axial seamount and from two locations on the eastern flank of the neovolcanic zone we recovered lavas with large (up to 1 cm) plagioclase crystals. One TV grab station recovered aphyric sheet flows containing abundant gabbroic xenoliths up to 8 cm in diameter with clinopyroxene to 8 mm and slightly smaller plagioclase crystals.

1.4.1.2. Geology and lava petrology of the large volcanic field at 8°50´S

The TOBI sidescan mapping during cruise M62/5A provided structural maps of the MAR between 7 and 12°S. Volcanic features can be very well distinguished and one of the largest and most interesting features in this segment is a volcanic field with a young appearance on the sidescan map. This volcanic field is defined based on a very similar reflectivity which is interpreted as lavas of approximately similar age in an area some 10 km long and 2 km wide. Large parts of the volcanic field consist of flat lava flows but at the western edge two rows of eruption centres are aligned in sigmoidal, about 3 km long lines probably overlying two major feeder dikes for the eruptions. Furthermore, several single volcanic features occur on the

volcanic field, most notable being an approximately 50 m high pancake shaped volcano with very steep cliffs. The sidescan map suggested a very young age of the lavas without obvious faults cutting the lavas. However, during the ROV dives we found some cracks and up to 15 m high faults running through the central part of the lava field implying that significant tectonic movements have occurred after ceasing of the volcanic activity, i.e. the segment probably is in a beginning tectonic rather than in a volcanic stage. The lavas are also covered by 1 to 2 cm thick carbonate pteropod/foraminifera ooze, especially in the central part whereas many lavas in the north appear to be less sedimented and younger. This may indicate a variable age of the different parts of the volcanic field.

Thirty samples of mostly glassy basalt were recovered by ROV dives and wax corer from various positions along the volcanic field. We especially sampled different small volcanic cones along the presumed eruption fissure in order to determine the heterogeneity of the erupting magmas. In contrast to the 4°48´S region the predominant lavas in the 8°50´S volcanic field are pillow lavas which appear to cover the central part whereas sheet flows are more abundant in the north. Here we observed frequent changes between pillows and sheet flows during station 159 (dive 44) and we also found collapse structures and lava pillars typical for fast eruptions. Consequently, the eruption volumes and the velocities must have varied with more lava erupting in the north.

1.4.1.3. Geology and lava petrology of the hydrothermal field at 9°33´S

The Lilliput hydrothermal field at about 9°33´S lies in the segment A3 which has a significantly thickened crust of about 11 km thickness based on gravimetric modelling (Minshull et al., 2003). The morphology of the A3 segment is reminiscent of the fast-spreading East Pacific Rise with a neovolcanic zone occurring on a shallow ridge with a narrow cleft rather than in a deep rift typical for the slow-spreading Mid-Atlantic Ridge. The cleft is some 900 m wide and 20 to 30 m deep with an about 10 m high volcanic ridge in the centre. The hydrothermal field lies in a water depth of about 1500 m in a pillow lava flow disrupted by several deep faults striking approximately 345°. South of the hydrothermal field we found very young-looking sheet flow lava flows suggesting that recent volcanic activity occurs in this part of the A3 segment. Possibly, these lava flows represent the heat source for the hydrothermal convection cells. Alternatively, the thick pillow flow itself may have initiated the hydrothermal circulation because hot water was observed to stream out of cracks in large pillows and most of the hydrothermal sediment is Fe-oxide/hydroxide crusts.

1.4.2. Description of hydrothermal precipitates

(S. Petersen, H. Paulick)

Hydrothermal precipitates were recovered from the Turtle Pits and Red Lion hydrothermal fields at 4°49’S as well as from the Liliput hydrothermal field at 9°33’S. The samples consist of massive sulfides, sulfide-oxide-sulfate breccias, and Fe-oxyhydroxides and are described below in detail. Major and trace element geochemical and mineralogical studies will be performed on these samples (S. Petersen, IFM-GEOMAR), as will be sulfur isotopic investigations (H. Strauss,

Uni Münster). Selected subsamples were taken for age dating in order to document variations with time (J. Scholten, Univ. Kiel). All samples will be archived at IFM-GEOMAR.

Note: Positions of the TV-grabs within the Turtle Pits field are preliminary and need to be recalculated!

Table 1.1: Hydrothermal precipitates

No.	Date / time	Lat / Long	Depth wire	comment
Turtle Pits				
114ROV-4	10.04.05/03:55	South Tower 4°48.579'S/ 12°22.420'W	2990 m	Black smoker chimney from SE base of tower (heading 336)
114ROV-5	10.04.05/04:15	South Tower 4°48.579'S/ 12°22.420'W	2990 m	Lower part of structure (heading 294)
114ROV-6	10.04.05/05:00	South Tower 4°48.579'S/ 12°22.420'W	2986 m	Near top of structure at western side (heading 084)
114ROV-7	10.04.05/05:09	South Tower 4°48.579'S/ 12°22.420'W	2986 m	Near top of structure at western side
123ROV-4	11.04.05/13:50	Marker 1 4°48.588'S/ 12°22.414'W	2986 m	Eastern side of Marker 1 chimney, sampled in bionet
123ROV-9	11.04.05/16:50	Pinoccio 4°48.562'S/ 12°22.419'W	2990 m	Small knob on western side of the inactive Pinochio chimney
124GTV	11.04.05/22:11	4°48.58'S/ 12°22.42'W	2998 m	1000 kg of massive pyrite (inactive chimney) sampled from sheet flow at western edge of the field
130ROV-1	13.04.05/14:39	Mk 2 BS 4°48.573'S/ 12°22.421'W	2985 m	Sampled in bionet during attempt to sample fauna
130ROV-2	13.04.05/14:57	Mk 2 BS 4°48.573'S/ 12°22.421'W	2985 m	Sampled in bionet during attempt to sample fauna
131GTV	13.04.05/21:05	4°48.57'S/ 12°22.37'W	2999 m	Fe-oxyhydroxide stained fresh basalt, plume fallout sampled in graben east of Pinoccio
139GTV	14.04.05/20:17	Mk 2 mound 4°48.573'S/ 12°22.421'W	2985 m	1000 kg of massive sulfide, hematite-magnetite-sulfate material, and chimney debris from western flank of Marker 2 mound
141ROV-6	15.04.05/	4°48.56'S/ 12°22.41'W	2985 m	Six pieces of pyrrhotite-rich chimney material
146ROV-3	16.04.05/20:24	4°47.90'S/ 12°22.62'W	3045 m	Inactive sulfide structure on the way to Red Lion
Red Lion				
146ROV-7	16.04.05/22:57	4°47.82'S/ 12°22.60'W	3048 m	Flange of Shrimp Farm in the Red Lion vent field
Liliput				
200ROV-5	25.04.05/13:01	9°32.93'S/ 13°12.51'W	1494 m	Fe-oxyhydroxide crusts
200ROV-7	25.04.05/15:48	9°32.88'S/ 13°12.55'W	1495 m	Fe-oxyhydroxide crusts
209GTV	26.04.05/14:53	9°32.86'S/ 13°12.52'W	1511 m	Fe-oxyhydroxide crusts, basalt glass chips and fauna
213GTV	27.04.05/01:58	9°32.83'S/ 13°12.55'W	1513 m	Fe-oxyhydroxide crusts, basalt glass chips and fauna
214GTV	27.04.05/03:55	9°32.84'S/ 13°12.54'W	1511 m	Fe-oxyhydroxide crusts, basalt glass chips and fauna

Turtle Pits area

Station 114ROV (dive#37):

During this dive chimney samples were recovered from the Southern Tower structure at Turtle Pits. The black smoker samples consist of porous chalcopyrite-rich pieces with minor pyrrhotite and pyrite/marcasite crusts of variable thickness. One sample (114ROV-5) is a larger peace from the trunk of the structure and is characterized by abundant pyrite, chalcopyrite and an anhydrite conduit within the pyrite crust. This seems to indicate that seafloor ingress into the structure is taking place and is channeled within the structure. Sample 114ROV-7 is a small knob of which the core consists entirely of pyrrhotite. A thin crust of pyrite and marcasite is also present.
Subsampling: SP=4C1, 4C2, 5B1, 5B2, 5G, 6, 7B; JSch=4B, 5B1, 7B; HS=5, 5C, 5bag, 6, 7.

Station 123ROV (dive#38):

Sample 123ROV-4 was taken on the eastern side of the Marker 1 black smoker complex and is the outer portion of an active chimney (Tmax at this site is close 400°C). The interior of the sample consists of chalcopyrite, pyrite and anhydrite. The outer portion is composed of a 1-5 mm marcasite crust and contains a few cm wide microchimneys on top. Exterior partly oxidized to Fe-oxyhydroxides plus white bacterial-associated globules (sulfur?). Sample 123ROV-9 was sampled at the inactive Pinoccio chimney and is strongly recrystallized. Subsampling: SP=4C1, 4C2, 9/3; JSch=9/3; HS=4A, 4B.

Station 124GTV:

This grab was aimed at sampling the sulfide mounds or inactive chimneys at the western flank of Turtle Pits. The target area was approached from the west and the grab was placed on top of a large sulfide boulder. Apon recovery it became evident, that this piece was a block of massive pyrite+/-marcasite with rare black sphalerite. Chalcopyrite is also rare, but slightly enriched in few samples near the interior of the sample. Ribbon texture is abundant in the outer parts of the structure indicating that this chimney was partially characterized by beehive textures. The samples have been grouped according to their texture. More massive samples belong to group 2, while samples characeterized by ribbon-like layering were grouped into group 3. Accidently recovered pieces of sheet flow basalt, representing the substrate on which the sulfide block was lying, are group 1. Subsampling: SP=2A2, 2B6, 2C3; JSch=2A3, 2B3; HS=2A6, 2B4, misc.

Station 130ROV (dive#40):

Few pieces of massive sulfide were co-sampled with the bionet (130ROV-1) and consist of two types of fragments: 1. Chimney interior consisting of anhydrite and chalcopyrite. 2. Chimney crust consisting of pyrite, chalcopyrite and marcasite, partially covered by Fe-oxihydroxides. Sample 130ROV-2 is a hollow chimney structure with 2 cm thick walls of chalcopyrite and marcasite. Interior of the vent (5 x 3 x 2 cm) is lined by 1-3 mm long beautiful bladed pyrrhotite crystals up to 1 mm in diameter. Subsampling: All to SP

Station 139GTV:

The station was targeted at the sulfide mound material of the Turtle Pits hydrothermal field. We approached the area from the west, passed a large boulder that was seen in some of the ROV-dives and placed the grab on the western flank of the Marker 2 mound.

The grab recovered close to 1000 kg of heterogenous sulfide-hematite-magnetite-sulfate material including small relict chimney conduit pipes (group 1), larger chimney pieces consisting of a chalcopyrite-rich interior and variably thick pyrite-marcasite rims (group 2). Sphalerite is a minor component in some of the samples as is late hematite+magnetite occurring as bladed infill in cavities and throughout some of the porous sulfides. Some of the inactive chimneys that were cosampled with the grab are dominated by massive friable chalcopyrite+/-pyrrhotite with only a thin py-mc crusts (group 3). Group 4 consist of gypsum-anhydrite-cemented samples and breccias with varying proportions of hematite, magnetite, chalcopyrite, and pyrite. Group 5 consits of very friable, soft grey material with abundant hematite+/-magnetite with associated greenish to yellow-white clay-like material (group 8). This material might well be talc, but only XRD-measurements will prove this. One primary chalcopyrite chimney is characterized by a rim of primary hydrothermal hematite-magnetite separating the interior from the pyrite-marcasite rim (group 6). Some of the anhydrite-cemented samples contain breccias of chalcopyrite conduits (mm to cm-sized) in sulfide sand that resemble conduit breccias in fossil massive sulfide depoits on land (group 7). Subsampling: SP=1A1, 2B2, 2C3, 3C3, 3D2, 3E5, 3H1, 4B2, 4C2, 4D11, 5A2, 5C3, 5D2, 5J2, 6A3, 6B2, 7B4, 7E5; JSch=2B23, 2C3, 3E5, 4D11, 5A2, 5D2; HS=2A3, 2B4, 2C2, 2E2, 2F3, 2G1, 3C1, 4A5, 4C4, 4D2, 4D7, 4G2, 4I, 5E2, 6B3, various gypsum needles.

Station 141ROV (dive#41):

The six pieces from sample 141ROV-6 consists of pyrite-marcasite crust with some chalcopyrite in the interior, which is typically altered (pigeon color). The redbrown outer surface is related to a thin Fe-oxihydroxide coating. One piece with central vug (2 x 3 cm) lined with pyrrhotite + isocubanite(?). Some of the fragments contain 1-3 mm layer of magnetite separating the chacopyrite and pyrite-marcasite zones. Subsampling: All to SP.

Red Lion area

Station 146ROV (dive#42):

Two sulfide samples were recovered during the transect from Turtle Pits into the rift valley and further north to the Red Lion site. Sample 146ROV-3 is a sulfide knob from an inactive chimney on the way north with a recrystallized interior with irregular cavities lined by sphalerite and chalcopyrite (crystals <1 mm). Bulk of the piece consists of chalcopyrite-marcasite. Crust: 2 mm black Fe-oxihydrixide. One sample was recovered from the Shrimp Farm chimney at the Red Lion hydrothermal field itself. It was sampled at the edge of a large flange and immidiately became a black smoker upon sampling. The sulfide contains abundant sphalerite. Internal cavitiy (2 x 1.5 cm) lined by pyrrhotite (+isocubanite?). A thin crust of pyrite/marcasite is extensively coated by white material (native sulfur?) and orange-brown Fe-oxides . Subsampling: SP=146-3, 146-7; HS=146-3.

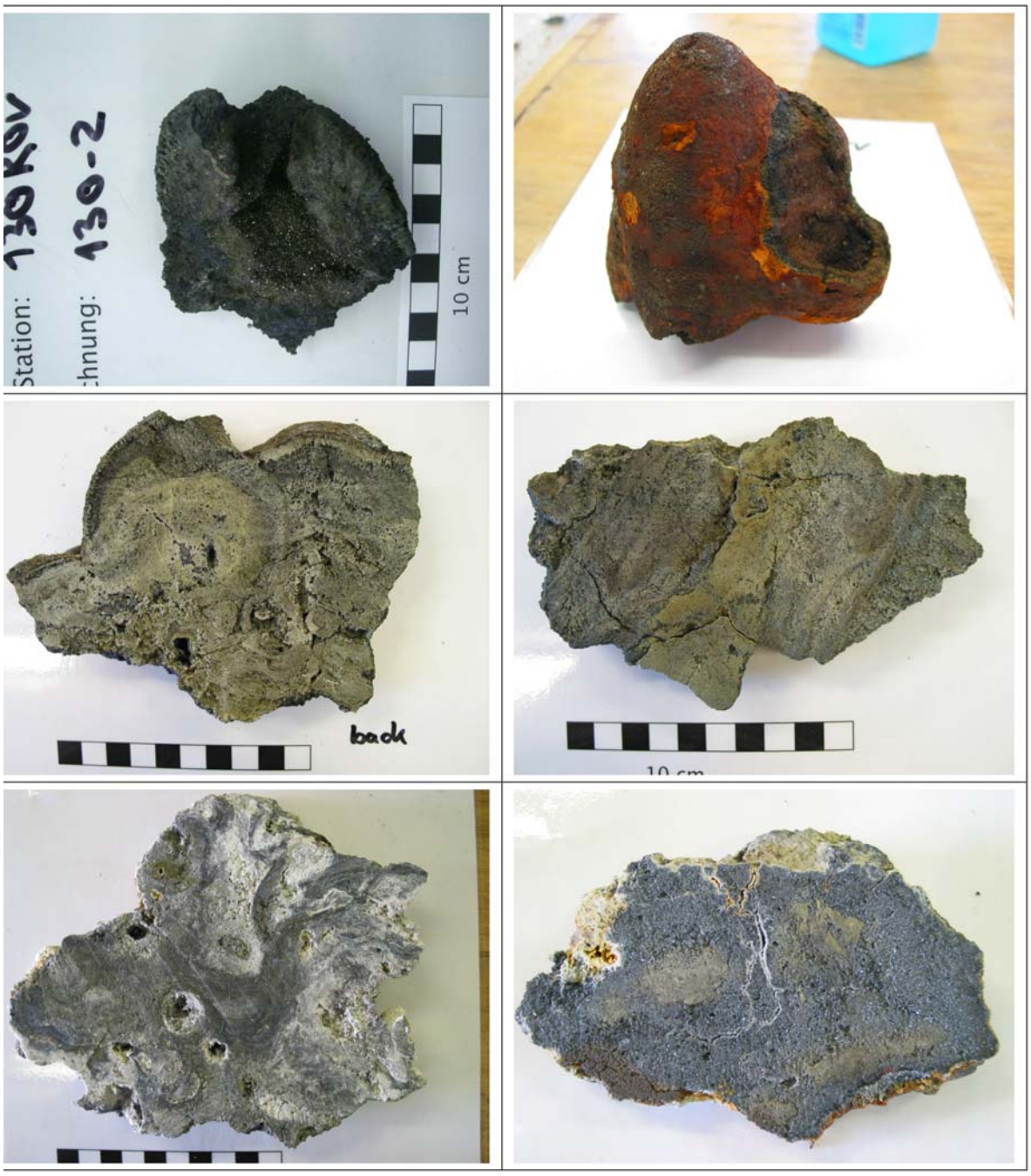

Figure 1.1: Selected samples from the Turtle Pits hydrothermal field. A) Active chimney conduit with bladed pyrrhotite in the core and a rim of pyrite/marcasite (sample 130ROV-2). B) Inactive chimney knob consisting of a chalcopyrite core, a pyrrhotite-rich zone and an outer rim of pyrite/marcasite stained red by Fe-oxyhydroxides (sample 139GTV-3A). C) Porous inactive chimney composed of pyrite wit a core of chalcopyrite. Multiple growth zones are visible. Late vugs are filled by black sphalerite (sample 139GTV-2F4). D) Massive pyrite cut by dense, recrystallized chalcopyrite. Fractures are lined with grey-metallic hematite-magnetite. E) Massive anhydrite/gypsum breccia with primary clasts of chalcopyrite and abundant grey hematite/magnetite. Individual conduits are lined by gypsum needles (sample 139GTV-4D6). F) Massive hematite/magnetite with relics of chalcopyrite+pyrite. This sample type is characterized by the lack of anhydrite and a clay-like alteration developed as a rim and along fractures (sample 139GTV5A3).

Liliput area

During three TV-grab stations (stations 209GTV, 213GTV, and 214GTV) and one ROV dive (200ROV) hydrothermal Fe-oxyhydroxide-rich crusts were sampled from the Liliput field. During sampling and upon recovery of the TV-grab it became evident that the Fe-oxyhydroxides are water-saturated muds with only thin crusts. These crusts desintegrated on sampling. In two of the grab stations thin sheets (<<1mm thick) of sulfides (pyrite/marcasite?) appeared. These might be the result of biological. Subsampling: All to SP. One piece of 209GTV to CF.

Fig. 1.2: Fe-oxyhydroxide crusts from the Liliput hydrothermal field, 9°33'S (sample 209GTV-2).

1.4.3. ROV and OFOS deployments

(H. Paulick, S. Petersen, K. Haase, S. Fretzdorff)

Turtle Pits

The Turtle Pits hydrothermal field is centered at 4°48.58'S / 12°22.42'W in a water depth of 2990 m and occurs within a fracture-controlled small depression. The fracture continues to the north and the south and is marked by aligned collapse pits within sheet flows. The central depression hosting the hydrothermal field is surrounded by sheet flows to the north and to the northwest, whereas jumbled flows are more exposed along the eastern side of the deposit. Turtle Pits itself consists of two mound areas (Marker 1 and Marker 2 sites) composed of sulfide debris with numerous small active black smokers at the top of the mounds (Fig.1.3) A 9.5 m high, active black smoker with vertical walls (Southern Tower) is located to the southeast of Marker 2 mound and is surrounded by a few small diameter black smoker orifice near its base. Two medium-sized inactive black smoker (Pinoccio and Stalagmite) as well as a third, more complex and somewhat older smoker, occur to the north of the active sites, where the central depression

narrows to within a few meters. Large toppled chimneys occur to the west of both the Marker 1 and Marker 2 sites, documenting previous periods of hydrothermal activity. Overall the deposit seems to be ~50 in length and up to 30 m wide. Exploration a couple 100 m to either side did not provide evidence for an extension of the deposit. Massive blocks of white (anhydrite-rich?) material are exposed along the northwestern side of the Marker 1 site. Smaller talus blocks of this material are transported into the pit to the east.

The **Red Lion** hydrothermal field lies is centered at 4°47.83'S/12°22.60'W (water depth of 3050 m) ~ 2 km north of the Turtle Pits field and consists of four active chimneys: Shrimp Farm, Zuckerhut, Mephisto, and Tannenbaum. These chimneys are between 4 and 6 m high and sit directly on a pillow lava floor. Three of the chimneys Tannenbaum, Zuckerhut, and Mephisto have a small pedestal of sulfide debris. Small (<0.5 m) inactive chimney are situated next to Shrimp's Farm and in the vicinity of Zuckerhut. Plume fallout is evident on the pillows in the immediate vicinity of the smoker. Two chimneys, Shrimp Farm and Zuckerhut are characterized by abundant shrimp responsible for the white colour of their tops. The most interesting aspect of these smokers is their flange growth, not commonly reported from seaflooor hydrothermal systems. The conductive cooling of the hydrothermal fluids through the flanges supports a thriving community of shrimp on these two structures. The other two chimneys do not show evidence for flange growth and shrimp are rare.

The distance between these two sites (Turtle Pits and Red Lion) may give evidence for the size of the individual hydrothermal convection cells in the area and provides a tool for the exploration of further sites in similar distance to those two hydrothermal field. This is supported by the discovery of small inactive sulfide deposits in the SW of the deposits suggesting, at least, a potential for additional vent sites in the area.

In addition to detailed investigations of the hydrothermal fields at 4°48'S, several ROV deployments were designed to investigate the volcanic geology of the MAR in detail (eruption-scale). The areas investigated are:

a) the neovolcanic zone between 4°47.76'S (Red Lion) and 4°48.90'S,
b) a „young" on-axis volcanic center at 8°40'S to 8°50'S (segment A2),
c) the surrounding of the Liliput hydrothermal field (9°33'S), and
d) on-axis and off-axis volcanic fields in the central A3 segment (9°34.40'S and 9°42.50'S).

Geological maps of these tracks are presented in Fig. 1.4 and in the following the principal observations are summarized.

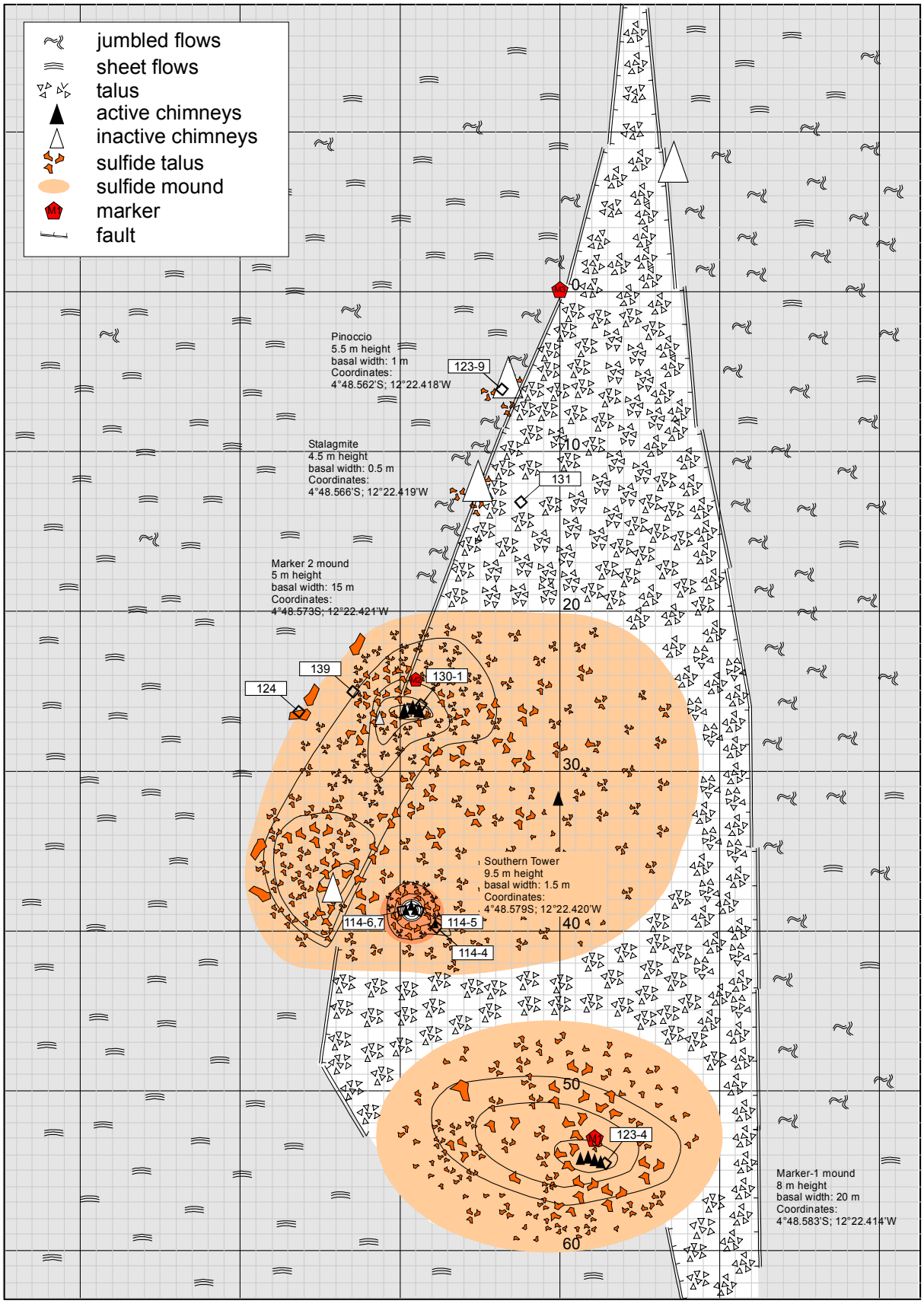

Fig. 1.3: Relative location of individual chimneys and mounds and geology around the Turtle Pits hydrothermal field, 4°48.58'S/12°22.42'W. Grid is 10 m.

Neovolcanic zone between 4°47.76'S (Red Lion) and 4°48.90'S

ROV dive 42 (station 146) transgressed ca. 800 m of the neovolcanic MAR at 4°48.90'S which consists mainly of fresh sheet flows including areas with jumbled and lobate flow textures. In contrast, a pillow mound (ca. 30 m high; radius >600 m) in the central portion of this MAR segment is heavily sedimented and locally dissected by tectonic faults indicating a relatively high age. To the north, the neovolcanic zone deepens significantly from 3005 m at 4°48.70'S to 3053 m at 4°47.80'S. Most of this area is dominated by fresh (no sediment cover) jumbled to lobate sheet flows, however, pillow lavas become increasingly abundant to the north. On these pillow flows an inactive black smoker chimney is located at 4°47.90'S and about 200 m further north the active black smokers of the Red Lion hydrothermal field were discovered.

On-axis volcanic center at 8°40'S to 8°50'S (A2 segment)

A relatively young volcanic center was identified in this area of the MAR (segment A2) during Meteor Cruise M62-5 based on side scan images which show highly reflective surfaces undisturbed by tectonic faulting and lineaments defined by coalesced volcanic edifices. The highly reflective surfaces have been interpreted as extensive young lava flows (sheet flows?) fed by voluminous fissure eruptions. Two ROV deployments (dive 43, station 155 and dive 44, station 159) were designed to ground truth these interpretations and obtain eruption scale samples of the basalts.

A 1500 m long transect started in the tectonized western margin of the MAR that consists of pillow basalt and talus breccia. The neovolcanic zone is ca. 900 m wide and characterized by sedimented pillow and lobate flows. The lobate flows are largely restricted to a 350 m wide area that rises by about 20 to 30 m above the surrounding pillow basalts and contact relationships indicate that this structure represents the youngest volcanic eruption. To the east, the terrain is characterized by abundant N-S trending tectonic faults marking the margin of the neovolcanic zone. The basalts sampled during this dive are aphyric to poorly olivine-phyric, providing little petrographic evidence for distinguishing the products of individual eruptions.

To the north, a ca. 1600 m portion of the neovolcanic zone has been investigated during dive 44 (station 159) which crossed a 400 m wide and 50 m high pillow mound. This mound consists of highly plagioclase-phyric basalt (10 vol% plagioclase phenocrysts up to 10 mm) and is covered by a thick blanket of white pelagic sediment that includes local patches of pteropoda shill. Furthermore, colonization by Gorgonaria is also prevalent. In contrast, the aphyric to poorly porphyritic basalt lava flows to the north and south of the pillow mound show only minor biological colonization and variable degrees of sedimentary cover suggesting a younger age. However, contact relationships at the base of the pillow mound are inconclusive in this regard.

Overall, the volcanic plain surrounding the pillow mound is dominated by lobate and ropy sheet flow morphologies including minor intervals with jumbled textures. About 500 m to the north of the mound, a pillow lava flow lacking a sedimentary cover is overlying a jumbled sheet flow. This pillow flow may represent the youngest volcanic eruption in the area.

Liliput hydrothermal field (9°33'S) and on-axis exploration (9°31.0'S to 9°33.20'S)

The Liliput hydrothermal field was discovered during ROV dive 47 (Station 200), which was targeted based on CH_4 anomalies in the water column. It consists of abundant, semi-lithified Fe-oxihydroxide accumulations over an area of some 100x40m and mussel colonies at 1495 m

water depth that form linear and patchy arrangements following pre-existing cracks and contacts in the underlying basalt pillows. Venting of warm hydrothermal fluids has been observed where cracks within individual pillows and intrapillow space provide primary permeability. Temperatures measured with the sensors mounted on the ROV at a distance of ca. 0.5 m from the vent sites peaked at 5.1 °C.

The Liliput hydrothermal field (9°32.85'S; 13°12.54'W) is located in the central zone of the neovolcanic MAR. The surrounding area is characterized by fresh, aphyric basalt pillow flows. To the west, there are abundant N-S trending escarpments flanking horst and graben structures. A strongly sedimented pillow mound with abundant Gorgonaria and other biological colonization marks the westernmost location visited during Station 200.

The OFOS track of Station 215 was designed to investigate the neovolcanic zone between 9°31.00'S and 9°33.22'S, an area where substantial CH_4 anomalies have been detected in the water column. In total, 800 images of the seafloor were taken at regular intervals of ca. 30 seconds and a CDT was mounted on the sledge. The entire area to the north of the Liliput field is dominated by pillow lavas with variable sediment cover and locally abundant cliffs and fissures marking the tectonized western margin of the neovolcanic zone. To the south of the Liliput field (9°33.00'S to 9°33.22'S) there are fresh pillow basalts and abundant mussels and light gray mats of hydrothermal (?) sediment were discovered at 9°33.20'S / 13°12.51'W (position of Meteor, cable length exceeds water depth by 20 m). This area may be the extension of the Liliput field along a N-S oriented lineament and represents an important target for further hydrothermal exploration.

On-axis and off-axis volcanic fields at 9°34.40'S and 9°42.50'S (A3 segment)

The central portion of the MAR between the Ascension and Bode Verde Fracture Zones (segment A3) is characterized by shallow water depths (reaching depths <1400 m), the absence of a deep central valley, and numerous off-axis volcanoes concentrated in an area to the east of the MAR (including Grattan Seamount). Two dives were targeted at investigating and sampling the on-axis neovolcanic zone (dive 46, Station 194) and the off-axis volcanic fields (dive 45, Station 188).

The neovolcanic zone at 9°34.38'S consists of about equal proportions of pillow flows and lobate to ropy sheet flows with prominent collapse structures. The basalts are aphyric and biological colonization is rare. The western flank of the active MAR at 13°13.70'W is marked by prominent N-S trending cliffs and the highest point in this area (1427 m) is ca. 50 m above the center of the neovolcanic zone (1470 m). This marginal zone consists exclusively of aphyric pillow basalts with abundant Gorgonaria and other fauna. The glass crusts of these basalts are extensively palagonitized and Mn-oxide/Fe-oxihydroxide coating is common. These observations indicate that the basalts on the western flank are older than the basalts in the neovolcanic zone. The off-axis volcanic fields have been studied at 9°42.50'S in an area located ca. 10 km to the east of the central MAR. Here, 20 to 30 m high pillow mounds are surrounded by extensive plains of white pelagic sediments (foraminiferous ooze) with localized and isolated outcrops of individual pillows and pillow ridges. Furthermore, there are tectonic escarpments with associated talus breccia. The aphyric to poorly porphyritic basalts show extensive palagonitization and coating by Mn-oxides and Fe-oxihydroxides, which, together with the locally abundant biological colonization, indicates that the volcanic activity is relatively old.

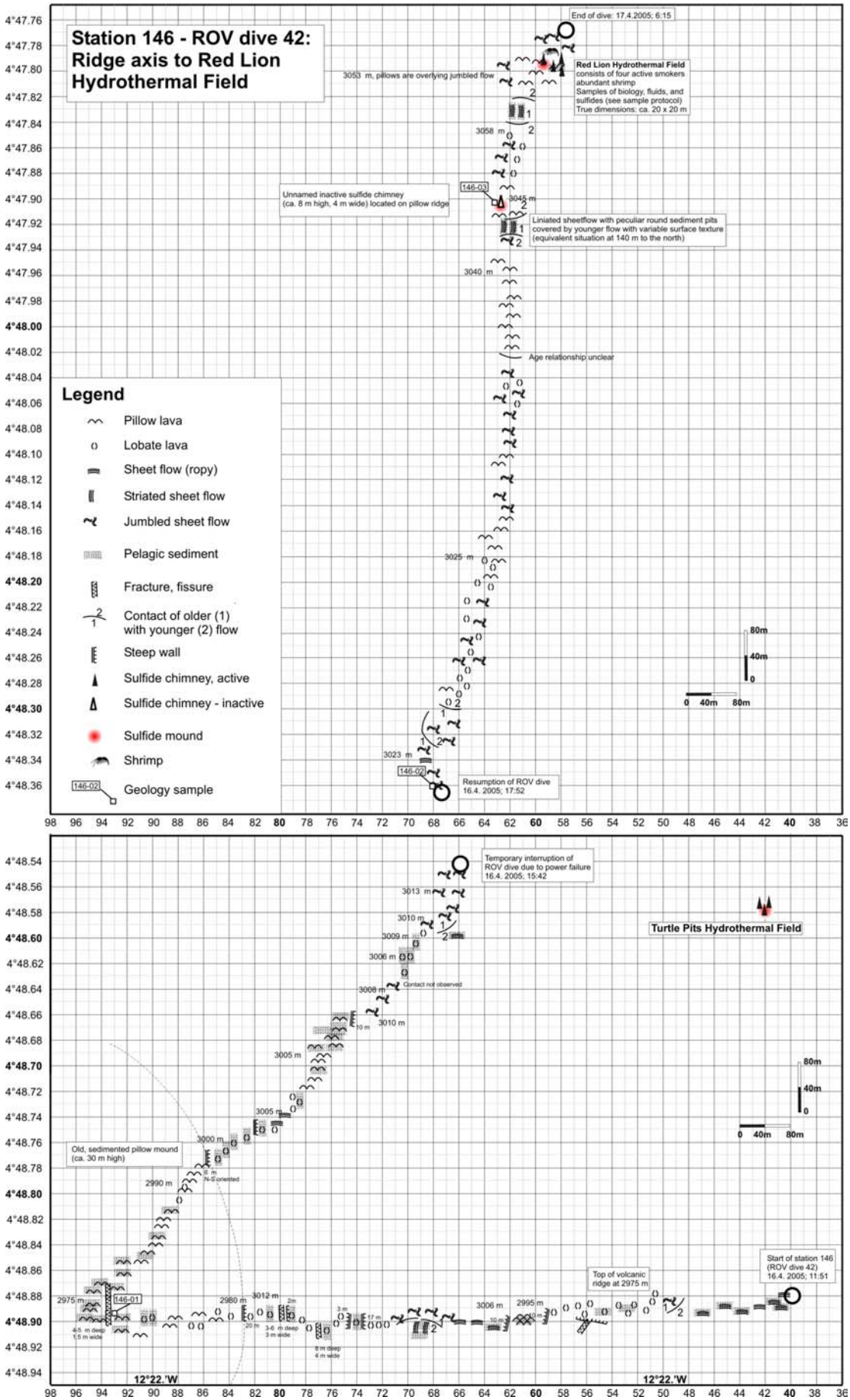
Station 146 - ROV dive 42:
Ridge axis to Red Lion Hydrothermal Field
End of dive: 17.4.2005; 6:15
Red Lion Hydrothermal Field
consists of four active smokers
abundant shrimp
Samples of biology, fluids, and sulfides (see sample protocol)
True dimensions: ca. 20 x 20 m
3053 m, pillows are overlying jumbled flow
3058 m
Unnamed inactive sulfide chimney
(ca. 8 m high, 4 m wide) located on pillow ridge
146-03
3045 m
Liniated sheetflow with peculiar round sediment pits
covered by younger flow with variable surface texture
(equivalent situation at 140 m to the north)
3040 m
Age relationship unclear
3025 m
3023 m
146-02
Resumption of ROV dive
16.4. 2005; 17:52
Legend
Pillow lava
Lobate lava
Sheet flow (ropy)
Striated sheet flow
Jumbled sheet flow
Pelagic sediment
Fracture, fissure
Contact of older (1) with younger (2) flow
Steep wall
Sulfide chimney, active
Sulfide chimney - inactive
Sulfide mound
Shrimp
Geology sample
80m
40m
0
0 40m 80m
Temporary interruption of
ROV dive due to power failure
16.4. 2005; 15:42
3013 m
3010 m
3009 m
3006 m
Contact not observed
3008 m
3010 m
3005 m
3005 m
3000 m
Old, sedimented pillow mound
(ca. 30 m high)
2990 m
N-S oriented
Turtle Pits Hydrothermal Field
Start of station 146
(ROV dive 42)
16.4. 2005; 11:51
Top of volcanic
ridge at 2975 m
2975 m
146-01
2980 m
3012 m
3006 m
2995 m
4-5 m deep
1.5 m wide
3-6 m deep
3 m wide
8 m deep
4 m wide
12°22.'W
12°22.'W

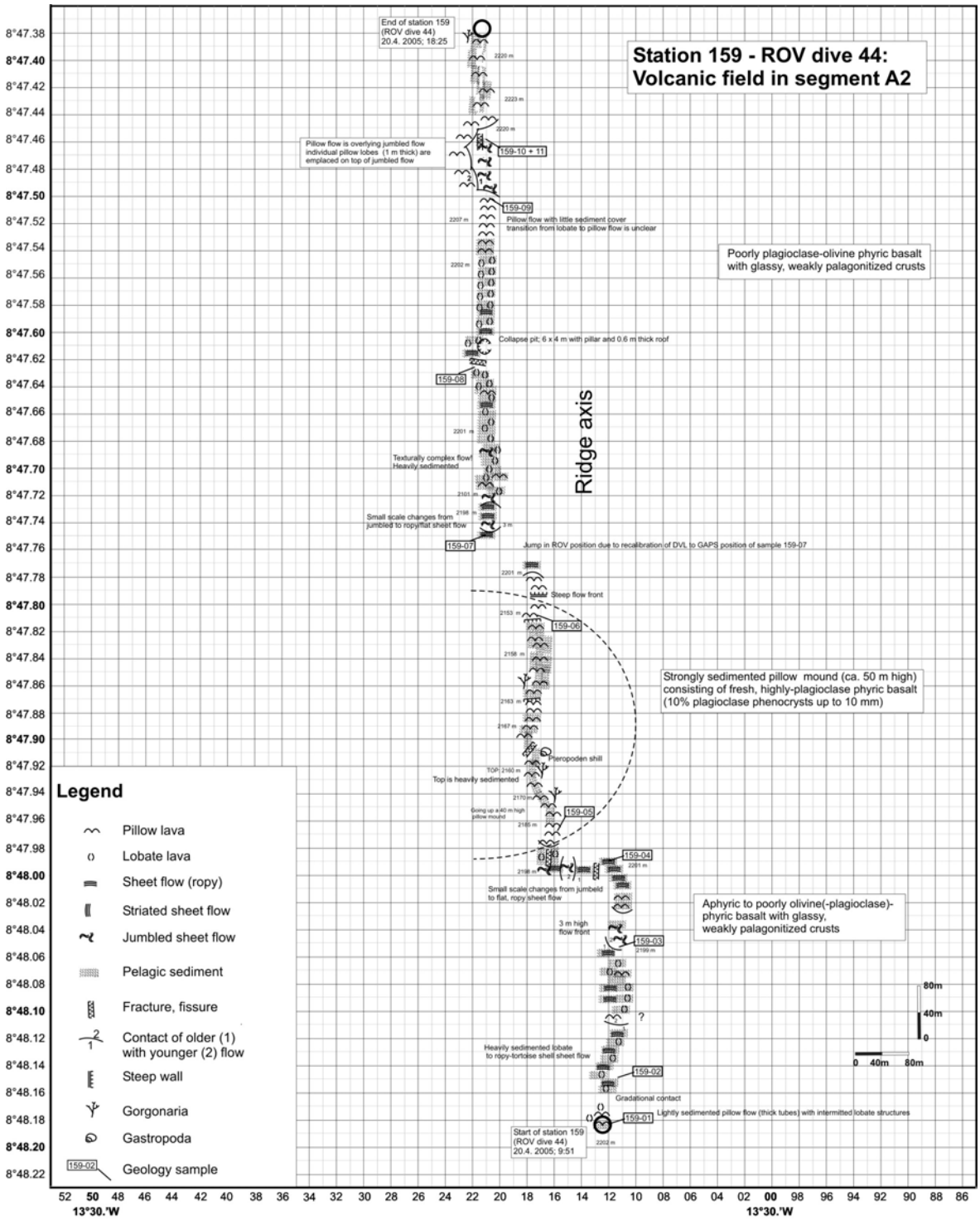
Station 159 - ROV dive 44:
Volcanic field in segment A2
End of station 159
(ROV dive 44)
20.4. 2005; 18:25
Pillow flow is overlying jumbled flow
individual pillow lobes (1 m thick) are
emplaced on top of jumbled flow
159-10 + 11
159-09
Pillow flow with little sediment cover
transition from lobate to pillow flow is unclear
Poorly plagioclase-olivine phyric basalt
with glassy, weakly palagonitized crusts
Collapse pit; 6 x 4 m with pillar and 0.6 m thick roof
159-08
Ridge axis
Texturally complex flow!
Heavily sedimented
Small scale changes from
jumbled to ropy/flat sheet flow
159-07
Jump in ROV position due to recalibration of DVL to GAPS position of sample 159-07
Steep flow front
159-06
Strongly sedimented pillow mound (ca. 50 m high)
consisting of fresh, highly-plagioclase phyric basalt
(10% plagioclase phenocrysts up to 10 mm)
Pteropoden shill
Top is heavily sedimented
159-05
159-04
Small scale changes from jumbeld
to flat, ropy sheet flow
Aphyric to poorly olivine(-plagioclase)-
phyric basalt with glassy,
weakly palagonitized crusts
3 m high
flow front
159-03
Heavily sedimented lobate
to ropy-tortoise shell sheet flow
159-02
Gradational contact
Lightly sedimented pillow flow (thick tubes) with intermitted lobate structures
159-01
Start of station 159
(ROV dive 44)
20.4. 2005; 9:51
Legend
Pillow lava
Lobate lava
Sheet flow (ropy)
Striated sheet flow
Jumbled sheet flow
Pelagic sediment
Fracture, fissure
Contact of older (1)
with younger (2) flow
Steep wall
Gorgonaria
Gastropoda
Geology sample
80m
40m
0
0 40m 80m
13°30.'W

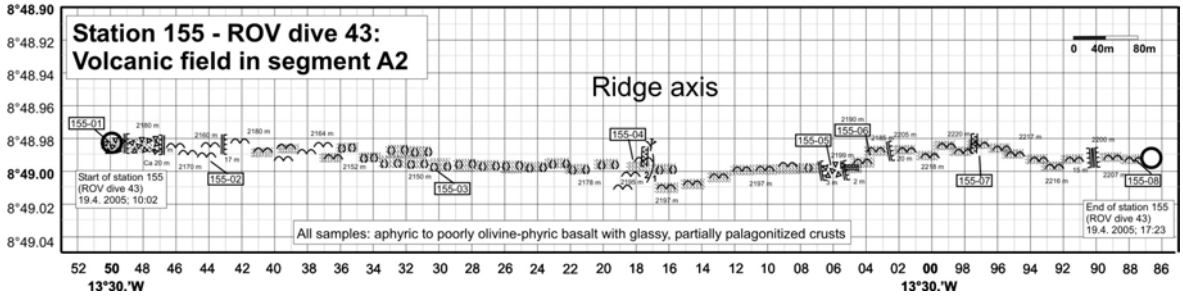
Station 155 - ROV dive 43:
Volcanic field in segment A2
Ridge axis
0 40m 80m
155-01
Start of station 155
(ROV dive 43)
19.4. 2005; 10:02
155-02
155-03
155-04
155-05
155-06
155-07
155-08
End of station 155
(ROV dive 43)
19.4. 2005; 17:23
All samples: aphyric to poorly olivine-phyric basalt with glassy, partially palagonitized crusts
13°30.'W

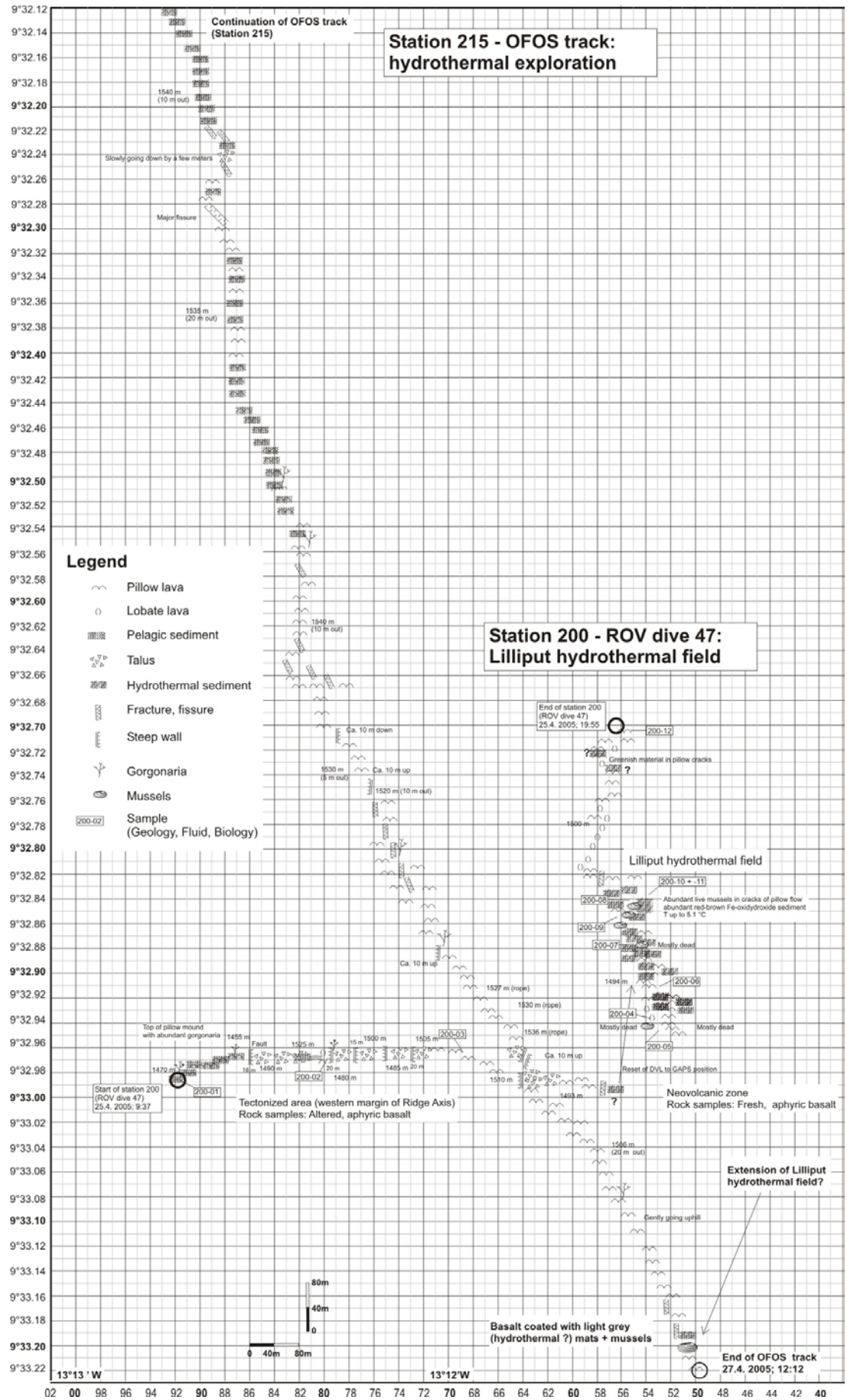
Station 215 - OFOS track: hydrothermal exploration
Continuation of OFOS track (Station 215)
Station 200 - ROV dive 47: Lilliput hydrothermal field
Legend
Pillow lava
Lobate lava
Pelagic sediment
Talus
Hydrothermal sediment
Fracture, fissure
Steep wall
Gorgonaria
Mussels
Sample (Geology, Fluid, Biology)
Lilliput hydrothermal field
Abundant live mussels in cracks of pillow flow
abundant red-brown Fe-oxidydroxide sediment
T up to 5.1 °C
Mostly dead
Greenish material in pillow cracks
Reset of DVL to GAPS position
Start of station 200 (ROV dive 47) 25.4. 2005; 9:37
End of station 200 (ROV dive 47) 25.4. 2005; 19:55
Top of pillow mound with abundant gorgonaria
Fault
Tectonized area (western margin of Ridge Axis)
Rock samples: Altered, aphyric basalt
Neovolcanic zone
Rock samples: Fresh, aphyric basalt
Extension of Lilliput hydrothermal field?
Gently going uphill
Basalt coated with light grey (hydrothermal ?) mats + mussels
End of OFOS track 27.4. 2005; 12:12
Slowly going down by a few meters
Major fissure
Ca. 10 m down
Ca. 10 m up
1540 m (10 m out)
1535 m (20 m out)
1549 m (10 m out)
1530 m (5 m out)
1520 m (10 m out)
1527 m (rope)
1530 m (rope)
1536 m (rope)
1493 m
1506 m (20 m out)
1494 m
1500 m
1455 m
1525 m
1500 m
1505 m
1490 m
1485 m
1480 m
1470 m
1530 m
200-01
200-02
200-03
200-04
200-05
200-06
200-07
200-08
200-09
200-10 + -11
200-12
80m
40m
0
0 40m 80m
13°13 ' W
13°12'W

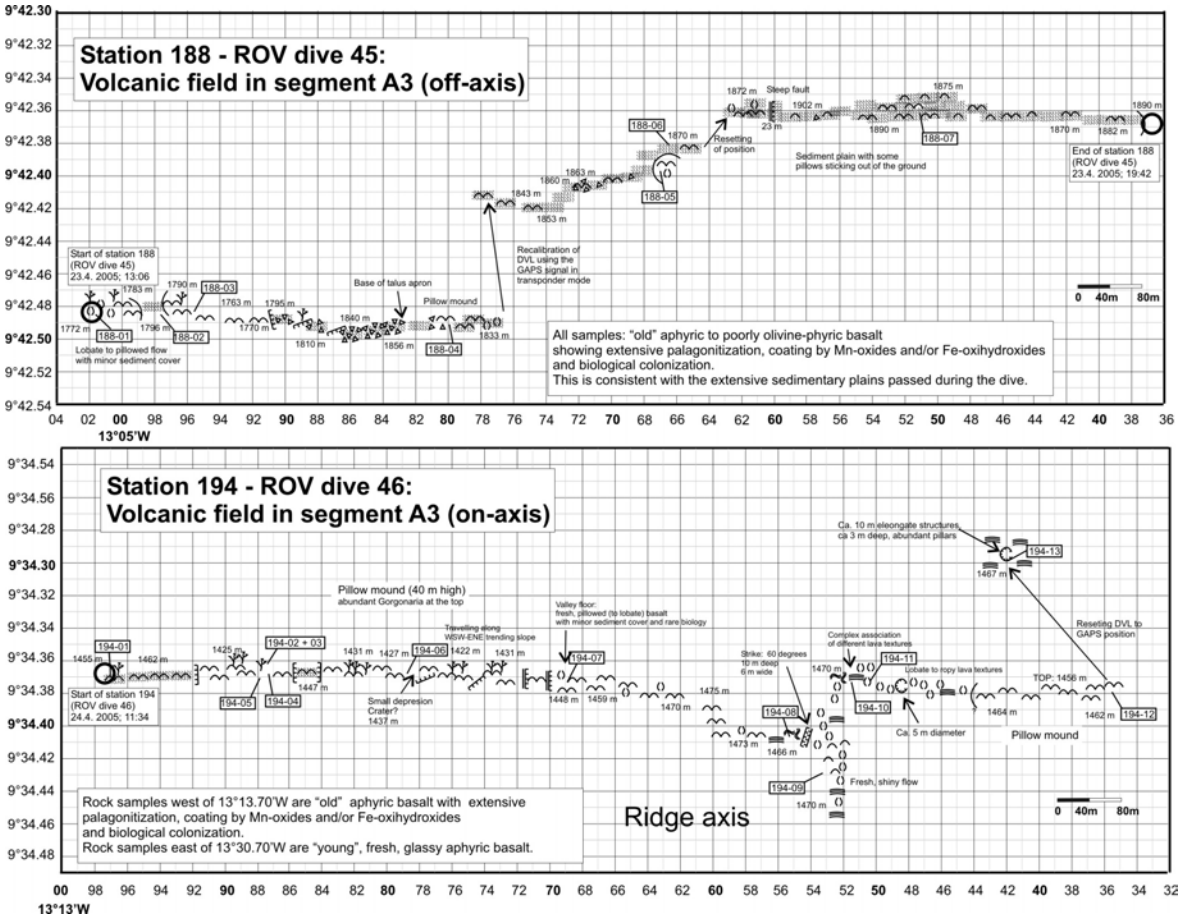

Fig. 1.4: Geology along ROV and OFOS tracks

1.4.4. Fluid Chemistry

(A. Koschinsky, H. Marbler, C. Ostertag-Henning, H. Strauss, U. Westernströer)

Hydrothermal fluids are characterized by their unique chemical and isotopic composition, which is significantly different from ambient seawater (e.g., van Damm, 2004). Scientific objectives for fluid chemical analyses, both on-board and subsequently in the home laboratories, include the detection of hydrothermal plumes in the water column and a quantification of the chemical and isotopic composition of hydrothermal fluids discharging from the ocean crust via distinct vent sites (either through black smokers or diffuse venting).

Three different types of samples were collected for chemical and isotopic analyses: water column samples from the CTD/Rosette, equipped with 24 bottles à 10 l volume; samples from discharging vent sites collected with three Niskin flasks (5 l volume), mounted at the front of the MARUM ROV QUEST; vent fluid samples collected with the new Kiel Pumping System (KIPS: 15 bottles à 675 ml) by inserting a titanium sampling nozzle into the orifice of smoker structures.

1.4.4.1. Fluid Sampling System for MARUM ROV QUEST

For sampling of hydrothermal fluids directly at the vent sites, a pumped flow-through system (Kiel Pumping System, KIPS) mounted on the ROV's starboard back side (Fig. 1.5) was used.

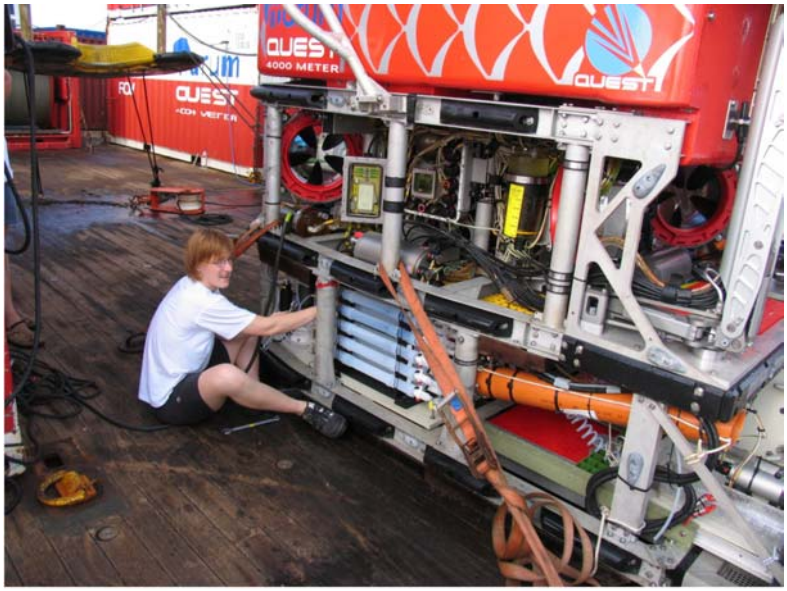

Fig. 1.5: The fluid sampling system "KIPS" mounted on the starboard back side of the Bremen MARUM ROV ("Quest") tool sled

The system was newly constructed and entirely made of inert materials (Teflon, titanium). Samples are collected via a titanium nozzle of 50 cm length which can be directly inserted into the vent orifice by the ROV`s manipulator arm. Parallel to the nozzle is a high-temperature probe measuring the *in situ*-sampling temperature. PFA tubing connects the nozzle to a 18 position-multiport valve motorized by a ROV actuator (SCHILLING, U.S.A) (Fig 1.6). The valve distributes the sample to max 15 individual PFA Teflon flasks with 675 ml volume each. Each bottle is equipped with all-Teflon checkvalves at inlet and outlet. All sample bottles are mounted in three racks A, B, C, with every rack containing five horizontally positioned bottles. For sub-sampling the three racks were transferred to the laboratory. A deep sea pump is mounted downstream to the sample bottles. The system is fully remotely controlled via the ROV control desk.

The system is modular in such a way that a number of bottles can be filled separatedly or interconnected in-line according to the needs of both sample volume and number of samples (c.f., leg M64/2). During leg M64/1 five sample flasks were filled at every sampling location,

thus, resulting in sufficient fluid volume (3.4 l) in order to study all aspects of fluid chemistry and dissolved gas composition on sub-samples that are as identical as possible. The bottles were pre-filled with freshwater or seawater. To assure the complete exchange of pre-filled water with sample fluid the total pumping time for 5 in-line bottles was determined experimentally. A total pumping time of 1 hour was applied during the cruise.

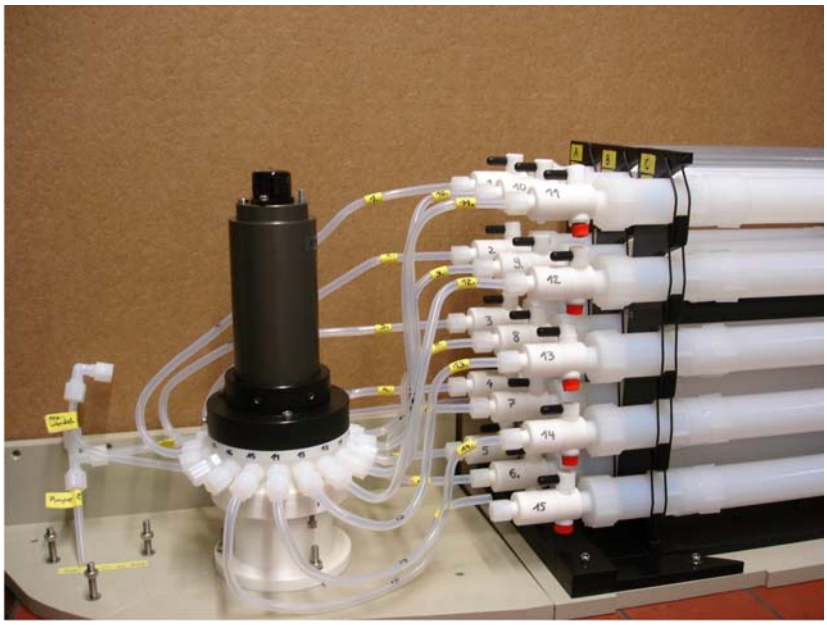

Fig. 1.6: Details of the Kiel fluid sampling system showing actuator-driven PETP multiport valve (left) and PFA tubing to 15 PFA Teflon sampling flasks in 3 racks A, B, C

1.4.4.2. Fluid Sampling and Sample Preparation

Water Column Samples

Based on the depth profiles for temperature, salinity and light transmission, samples were collected at different depths with the CTD/Rosette system, covering the vertical distribution of the hydrothermal plume. Sampling of these waters was performed directly after recovery of the CTD/Rosette system.

Immediately after sampling, pH and Eh were measured. Subsequently, and depending upon future chemical analyses, non-filtered subsamples (with aliquots either non-acidified or acidified to a pH of 2 with suprapure HCl) were stored at 4°C.

Barium sulphate was precipitated from sample aliquots (addition of barium chloride solution at pH 2) for measuring the sulphur and oxygen isotopic compositions of dissolved sulphate. For selected CTD stations, untreated water samples were collected for measuring the oxygen and hydrogen isotopic composition of these waters.

For the CTD stations in the vicinity of the Turtle Pits, Wideawake Mussel Field and Red Lion hydrothermal fields, samples throughout the water column have been collected for the analysis of amino acids in the dissolved and particulate organic material. Water samples were filtered through GF/F glass fibre filters and the filters wrapped in aluminium foil and frozen at -20°C. The organic compounds in the filtrate were concentrated by means of solid phase extraction onto C18 and SCX phases and subsequently stored at -20°C. For selected profiles throughout the water column an aliquot of the samples has been frozen at -20°C for later analysis of the ammonium concentration and its nitrogen isotopic composition.

Vent Fluid Samples

Immediately after recovery of the ROV, all three Niskin flasks (N1, N2, N3) and all bottles from the KIPS were sub-sampled. On small aliquots (20 ml), ph and Eh were measured directly after sampling for all samples.

Aliquots were sub-sampled for the following chemical and isotopic analyses: major and trace elements, selected anions, methane and hydrogen (abundance and isotopic composition), sulphate and sulphide sulphur isotope geochemistry, dissolved inorganic carbon (abundance and isotopic composition), amino acids, ammonium (abundance and nitrogen isotopes).

Unfiltered sample aliquots were collected for gas chemistry, for analyses of dissolved sulphide, for dissolved inorganic carbon, for amino acid analyses, and for ammonium measurements. Similarly, unfiltered water was sub-sampled for microbiological work.

For all other chemical analyses, fluid samples were pressure-filtrated with Nitrogen (99.999%) at 0.5 bar through pre-cleaned 0.2 µm Nuclepore PC membrane filters by means of polycarbonate filtration units (Sartorius, Germany). The filtrates were separated into aliquots for voltammetric and ICP analyses and acidified to pH 1 with 100 µl subboiled concentrated nitric acid per 50 ml (ICP) and with suprapure HCl to pH 2 (voltammetry), respectively. For selected samples, about 150 ml of fluid were filled into specially pre-cleaned bottles and immediately deep-frozen at -20°C. These samples are shipped in frozen state for the determination of organic metal complexation in the home laboratory of the project partner Dr. Sylvia Sander (University of Otago, New Zealand). Some representative samples were deep-frozen or poisoned with $HgCl_2$, respectively, as conservation for organic analyses in the home laboratory.

Procedural blanks were processed in regular intervals. All work was done in a class 100 clean bench (Slee, Germany) using only all-plastic labware (polypropylene, polycarbonate, PFAteflon). Rinse water was ultrapure (>18.2 Mohm), dispensed from a Millipore Milli-Q system.

A total of 227 water column samples, 26 bottle samples from the fluid sampling system, and 17 Niskin samples were collected. After return to the home labs, in Kiel selected samples will be analysed for major (Mg, Ca, Ba, Sr, Na, K, Si, Fe, Mn, B, Cl) and trace element composition (e.g., I, Br, Li, Al, Cs, Ba, Sr, Y-REE, Fe, Mn, Cr, V, Cu, Co, Ni, Pb, U, Mo, As, Sb, W, PGE) by ICP-OES (Spectro Ciros SOP CCD) and ICP-MS using both collision-cell quadrupole (Agilent 7500cs) and high-resolution sector-field based instrumentation (Micromass PlasmaTrace2).

At IUB in Bremen, voltammetry will be used for further trace metal analyses (Zn, Cd, Pb, Cu, Co, Ni, Ti, V, Mo, U, Tl, Pt). ICP-MS and ICP-OES measurements of minor elements and trace metals (see above) will be carried out as well for interlaboratory comparison. Li and Na will be analysed by flame photometry, and photometric methods will be used to determine anionic compounds (silicate, phosphate, sulfate, chloride). The duplicate coverage of some elements with different methods will be used for the evaluation of the methods and the data. The determination of organic complexation of Fe, Cu, and Zn (S. Sander, Univ. Otago) will be done by voltammetric ligand titration.

At the Westfälische Wilhelms-Universität Münster, sulphur (sulphides, sulphates), oxygen (sulphates, fluid samples), and hydrogen (fluid samples) isotope measurements will be performed.

At the Bundesanstalt für Geowissenschaften und Rohstoffe (BGR) in Hannover the amino acid concentrations (HPLC-FD) and their racemization (GC-FID) as well as their isotopic composition (GC-irmMS) will be analysed for selected samples. Additionally, the ammonium concentration and its nitrogen isotopic composition will be investigated. For a set of samples the concentration and carbon isotopic composition of the dissolved inorganic carbon will be analysed by a Finnigan Gasbench-Delta Plus-MS coupling.

1.4.4.3. On-board analyses

pH and Eh Measurements

For all samples collected with the CTD/Rosette, the Niskin flasks and the Kiel Fluid Pumping System, pH and Eh measurements were performed on unfiltered sample aliquots immediately after sampling. Measurements were carried out with WTW electrodes (Ag/AgCl reference electrode).

Chloride Titration

In order to determine whether or not phase separation affected the chemical composition of the hydrothermal fluids, respective fluid samples collected during ROV dives, either with Niskin bottles or with the Kiel Fluid Sampling System, were subjected to chloride concentration analysis. Measurements were performed as titration with 0.1 mM $AgNO_3$-solution, using fluorescene-sodium as the indicator. For reference, samples from a water column profile were also analyzed.

Photometric Determination of Dissolved Inorganic Silica

Silica tends to be enriched in hydrothermal fluids (e.g., van Damm, 2004). Hence, fluid samples and selected CDT/Rosette water column samples were analyzed for their abundance of dissolved silica. The analysis of dissolved silicon compounds in seawater and hydrothermal fluids is based on the formation of α-silicomolybdic acid via complexation of the dissolved silica with ammoniumheptamolybdate (e.g., Grasshoff et al., 1999). Concentration measurements were performed with a biochrom Libra S12 spectral photometer at an extinction of 810 nm. Silica contents in water column samples were measured both in filtered and non-filtered samples. No significant difference was detected.

Photometric Determination of Iron Concentrations

The principle of this method is the determination of an orange-red ferroin complex, which is formed by Fe(II) ions in the fluid sample with 1,10-phenantroline in a pH range of 3-5. In addition to a quantification of Fe(II), it is also possible to measure the Fe_{tot} fraction in the sample by reducing all Fe with ascorbic acid. Fe(III) is determined as difference between Fe_{tot} and Fe(II). Analyses were carried out with a biochrom Libra S12 spectral photometer and the absorption was measured at 511 nm. Fe concentrations were measured only in filtered samples of hydrothermal fluids. The detection limit is about 0.1 ppm. Samples with concentrations above 100 ppm were measured in diluted samples.

Voltammetric Determination of Trace Element Concentrations

For onboard sulfide and trace metal concentration analyses, the electrochemical method of voltammetry was used. Voltammetry is able to differentiate between different redox species and (in combination with UV digestion of the water samples) free and complexed forms of ions in

solution and is highly sensitive. All the voltammetric measurements were performed using a Metrohm system comprising a 757 VA Computrace run with a standard PC, an 813 Compact Autosampler and two 765 Dosimats. The three-electrode configuration consisted of the multi-mode electrode (MME) as the working electrode, an Ag/AgCl reference electrode (3 mol l^{-1} KCl), and a platinum wire as the auxiliary electrode.

Immediately after recovery, the unfiltered fluid samples were analysed for total dissolved sulfide in alkaline solution using the method after Metrohm Application Bulletin 199/3e. Filtered aliquots were submitted to a digestion process in a UV Digestor (Model 705, Metrohm), which contains a high pressure mercury lamp (500 W), decomposing organic metal complexes. After 1 hour UV irradiation, the total content of Fe and Mn in all samples and of Zn, Cu, Cd, and Pb in selected samples were determined by the standard addition method. For Fe, the highly sensitive cathodic stripping voltammetric method of Obata and van den Berg (2001) using 2,3-dihydroxinaphthalene as complexing agent was applied in samples with low Fe concentrations, while photometry was used for samples with high Fe concentrations (>0.1 ppm). Mn concentrations were determined using anodic stripping voltammetry in an alkaline ammonia buffer solution (Locatelle and Torsi, 2001). For Cu, Pb, Cd, and Zn analyses samples were buffered at pH 4.6 with 1 M acetate buffer solution and measured by ASV (Application Bulletin Metrohm 231/2).

1.4.4.4. Results from On-Board Analyses

Vent Fluids

The chemical and isotopic characterization of hydrothermal vent fluids is strongly dependent upon the sampling procedure. Dilution with ambient seawater is always likely. In order to qualitatively assess the contribution from seawater, a number of analytical parameters, such as Eh, chloride have been measured on-board. A final quantification of the fluid contribution from a hydrothermal source will be performed by using Mg concentrations (hydrothermal endmember Mg = 0, seawater endmember Mg = 55 mM). These will be measured in the home laboratory.

The pH and Eh measurements for the samples collected directly at the vent sites during ROV deployments clearly reflect the mixture of hot reducing hydrothermal endmember fluid and oxic seawater. Lowest values for the hydrothermally purest samples were 3.83 for pH and –260 mV for Eh. A crossplot of respective data (Fig. 1.7) allows a clear distinction between hydrothermal fluid and seawater. Most extreme values have been measured for samples from the Turtle Pits area (ROV stations 141 and 146). Results obtained from Niskin flask samples are somewhat in between both endmembers, i.e. reducing hydrothermal fluid and oxidized seawater.

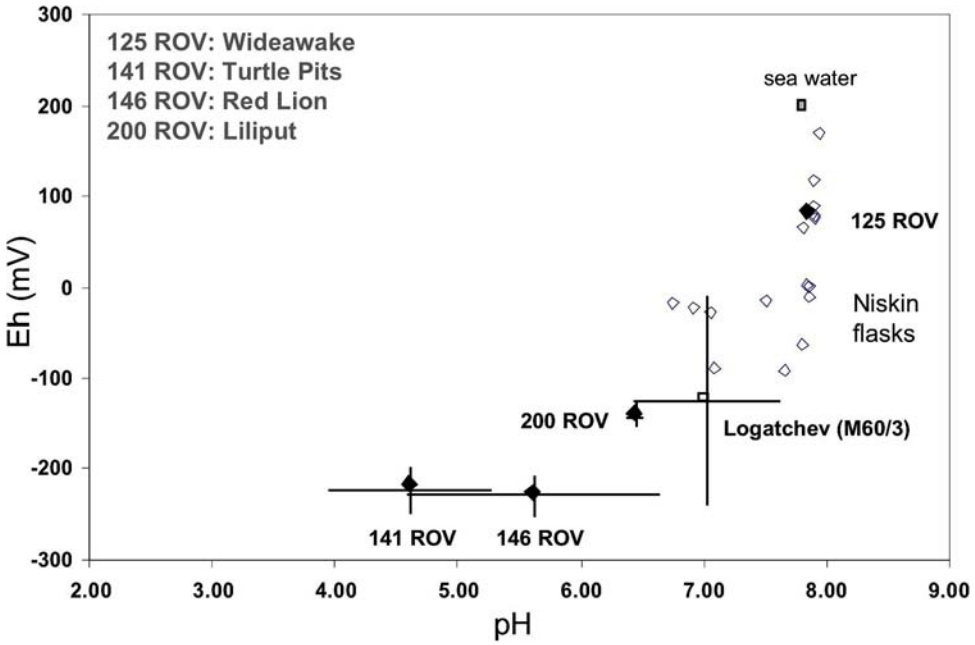

Fig. 1.7. Crossplot of pH and Eh for fluid samples from Niskin flasks and KIPS bottles

Measured sulfide concentrations were less than 1 mg/L in all samples, which may be partly due to the loss of free sulfide through Fe sulfide precipitation during cooling of the hydrothermal fluids. Chloride titrations indicated that the hot vents from the Turtle Pits field have significantly reduced chloride concentrations (minimum value at 13.52 mg/L) compared to a background seawater value of 21.0 mg/L. This clearly indicates that the fluids are phase-separated and that the samples represent the vapor-type phase. Silica is up to 200fold enriched over an average seawater concentration of about 1 mg/L. Si enrichment is typical for hot hydrothermal fluids (as exemplified by samples from ROV stations 141 and 146) due to intensive water-rock interaction. The same applies to Fe and Mn, having highest concentrations of dissolved total Fe of up to 105 mg/L, of which more than 80 % were found to be Fe(II), and up to 0.9 mg/L Mn. It has to be noted that the endmember concentration of Fe, including all Fe bound in the sulfide particles, is significantly higher, but can only be determined later in the home laboratory. Very low concentrations of dissolved Zn (max. 30 µg/L), Cu (max. 7 µg/L), Pb, and Cd were detected, indicating that most of these chalcophilic elements, which are typically enriched in hydrothermal fluids, are strongly bound into the precipitating sulfide particles, parallel to Fe.

Diffuse vent fluids collected from the Liliput hydrothermal field at 9°33'S are characterized by moderate enrichment of elements that were found to be high in the hot fluids, confirming their mixed fluid – seawater character. They were also significantly reducing (Eh of -137 mV) with slightly lowered pH (6.5).

Water Column Profiles

As Eh measurements are a fast and relatively simple analytical tool, they were used as the first measurement following the recovery of CTD water column samples in order to search for hydrothermal plume indications. For several stations, Eh minima clearly correlate with maxima of other hydrothermal tracers analysed, such as methane, hydrogen, Mn, and Fe concentrations (Fig. 1.8). However, especially when the plume signals were not very pronounced, Eh anomalies

were less pronounced or absent. Mn and Fe, were both detected in concentrations significantly above ambient seawater background in samples with very high methane and hydrogen concentrations and from the depth range with high turbidity values. In contrast, respective enrichments could not be detected in samples with lower gas concentrations. This observation can be used as an indicator for the proximity of the source, because the CH_4/Mn or CH_4/Fe ratios typically increase away from the plume due to metal oxidation and particle fallout. As Fe and Mn were determined in unfiltered samples, the data represent total dissolvable concentrations.

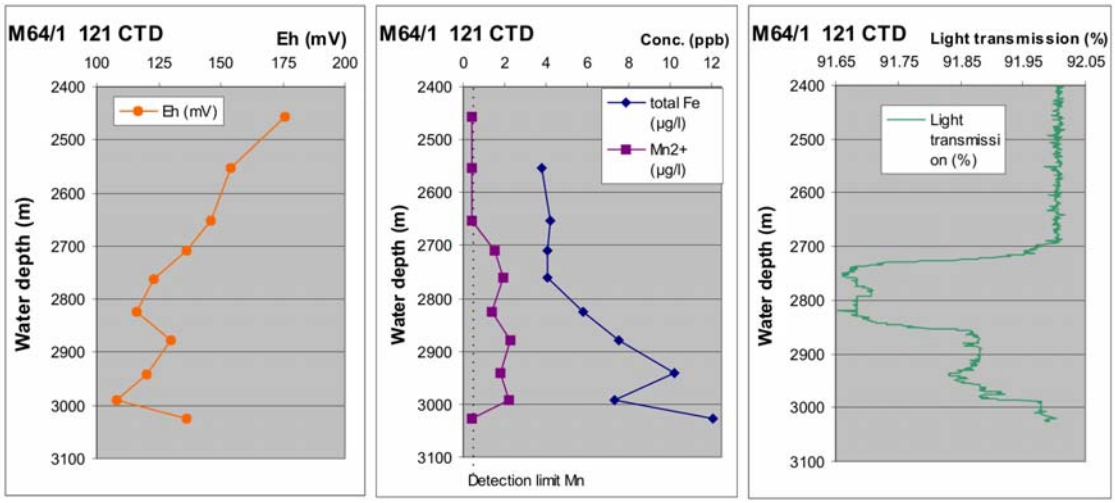

Fig. 1.8 Water column profiles of hydrothermal tracers, indicating the existence of a hydrothermal plume between 2700 and 3000 m water depth at 5°S

1.4.5. Dissolved Gases and Carbon Species

(R. Seifert, S. Weber, M. Warmuth)

1.4.5.1. Introduction

Objective of the work during M64/1 was to localise and characterise hydrothermal fluids and plumes using *in situ* sensors (CTD with sensors for redox and light transmission) and applying on board analytical techniques to determine concentrations of dissolved reactive gases (CH_4, H_2). To elucidate the transformation of carbon species and reduced gases brought along by hydrothermal fluids, a comprehensive set of samples was secured for on shore analysis of stable isotope contributions (H, C, He) of fluid components. Subjects of the study were hydrothermal fluids and plumes of two areas along the MAR - Red Lion / Turtle Pits / Wideawake (04°48'S), and the Liliput hyrothermal field (9°30'S) with the latter discovered during this cruise.

For this purpose 39 stations were covered by CTD/Rosette and a total of 252 water samples were obtained from these CTD stations and 6 ROV stations.

1.4.5.2. Samples and Methodology

CTD data were recorded using a SEABIRD CTD Type 911 equipped with a Eh sensor (AMT series 40) and a sonsor for light transmission as well as a rosette of 24 10L Niskin bottles. Water

samples were taken during lifting keeping the sampler at a certain depth for a short time. A total of 39 stations were performed of which only did failed to yield data. At 107 CTD misfunction of the temperature sensor occurred at about 1100m water depth caused by seawater entrance at the connection to the data transfer unit. The problem could easily be solved. Data of station 129 CTD were lost by a problem with data recording system on deck. For all other stations data could be recorded and saved for the entire water column.

Light dissolved hydrocarbons were analysed on board applying a purge and trap technique (Seifert et al., 1991). The water sample is stripped by He and analyses in the outflowing gas stream are concentrated in cooled traps at -84°C. After degassing, the trapped gases are released to a gaschromatograph (CARLO ERBA GC 6000) equipped with a packed (activated Al_2O_3) stainless steel column and a flame ionisation detector (FID) to separate, detect and quantify individual components. Recording and calculation of results is performed using a PC operated integration system (BRUKER Chrom Star). Analytical procedures were calibrated daily with commercial gas standards (LINDE). Analyses were generally done within 12 hrs after sampling.

For on board *measurements of dissolved hydrogen* up to 615ml of sample is connected to a high grade vacuum in an ultrasonic bath and heated until boiling. Aliquots of the released gas are transferred via a septum from the degassing unit into the analytical system. A gaschromatograph (THERMO TRACE) equipped with a packed stainless steel column (Molecular sieve 5A, carrier gas: He) and a pulsed discharge detector (PDD) is used to separate, detect and quantify Hydrogen. Recording and calculation of results is performed using a PC operated integration system (THERMO CHROM CARD A/D). Analytical procedures were calibrated daily with commercial gas standard (LINDE).

For on shore measurements of the *He concentrations and isotopic signature*, water samples were taken immediately after finishing the respective station. The samples were sealed head space free and gastight in copper tubes. Measurements will be performed at the Universität Bremen, Fachbereich 1 (Tracer Oceanography).

Samples for the determination of $\delta^{13}C$ *of the dissolved light hydrocarbons* were obtained by degassing the water samples with a vacuum - ultrasonic technique (see above). Aliquots of the released gas were transferred via a septum from the degassing unit into gastight glass ampoules filled with NaCl-saturated water for on shore analysis by GC-Isotope-Ratio-Mass-Spectrometry.

For on shore analysis of *stable carbon isotopes of dissolved inorganic carbon (DIC)*, aliquots of unfiltered sample was spiked with NaOH and BaCl2 directly after recovery to precipitate carbonate species. The analyses of $\delta^{13}C$-DIC will be made by Dual-Inlet-Isotope-Ratio Mass-Spectrometry (THERMO MAT 252).

For on shore analysis of *stable isotopes for dissolved hydrogen*, up to 10mL of gas obtained by vacuum/ultrasonic degassing of sample was frozen on molecular sieve 4A under liquid nitrogen in a pre-vacuated glass vial. The samples will be analysed via a molecular sieve 5A PLOT column and a GC-Isotope-Ratio-Mass-Spectrometer for $\delta^{2}H$-vlues.

To obtain an overview on the organic components contained in the hydrothermal fluids, selected samples were treated by Solid Phase Extraction (SPE).

1.4.5.3. Results

For the first working area (Turtle Pits, Red Lion, Wideawake) Most CTD profiles obtained in revealed imprints of hydrothermal activity within the water column by anomalies in the transmission profiles and ST diagrams (salinity versus potential temperature). These anomalies were present at a water depth range from 2700 to 3000m (Fig. 1). The S/T plots evidence the intrusion of a component relatively depleted in salinity.

Results for concentrations of dissolved methane and hydrogen obtained from CTD/rosette samples on board RV METEOR revealed hydrothermal signatures within the same depth range but do not correlate well with each other and the observed light transmission anomalies (Fig. 2).

Samples obtained by ROV directly at the fluid emanations revealed very high concentrations of dissolved hydrogen and Methane. Maximum concentrations found accounted for 0.29 mmol L^{-1} and 0.02 mmol L^{-1} of hydrogen and methane, respectively. The sample was obtained by putting the tip of the fluid sampling system directly into the outlet a black smoker vigorously exhaling boiling fluid (Station 41 ROV; Turtle Pits). The resulting H_2/CH_4 ratio of about 14.7 (Fig. 3), that is also found in water samples taken by ROV-based Niskin bottles in the vicinity of the smoker, even exceeds those we found for fluids of the Logachev field (see Table 1.2). A higher ratio is so far only reported for fluids obtained at the EPR at 21°N (Welhan & Craig, 1979). A fluid sample recovered from a black smoker within the Red Lion hydrothermal field (146 ROV) revealed H_2/CH_4 ratio of about 3 with concentrations of CH_4 and H_2 of 26 µmol L^{-1} and 75 µmol L^{-1}, respectively. More precise data on the differences of gas concentrations will only be available after having determined the fluid – seawater mixing ratios. The two sampling locations are about 2 km apart and harbour considerably different vent faunas. More information on the factors holding responsible for the different fluid compositions are expected from on shore analyses of stable isotope signatures and trace metal content. However, the data already available illustrate the presence of compositional distinct black smoker vent fluids and faunas within a relatively narrow area at 04°48’S.

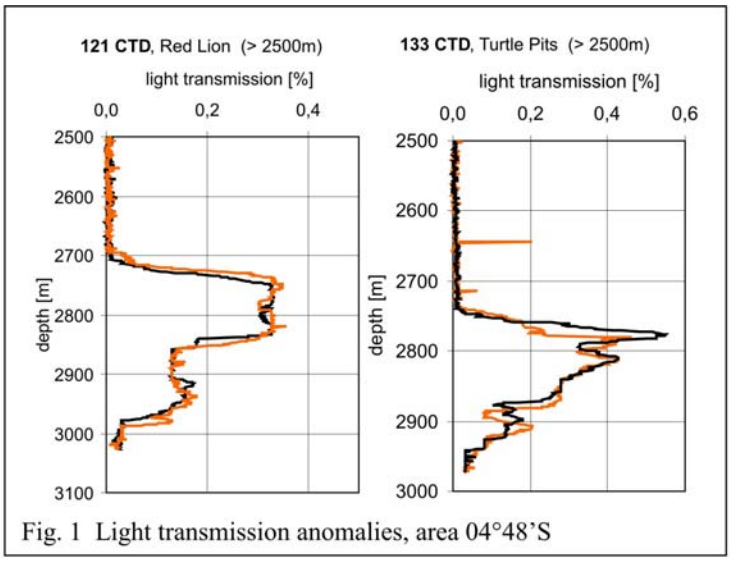

Fig. 1 Light transmission anomalies, area 04°48'S

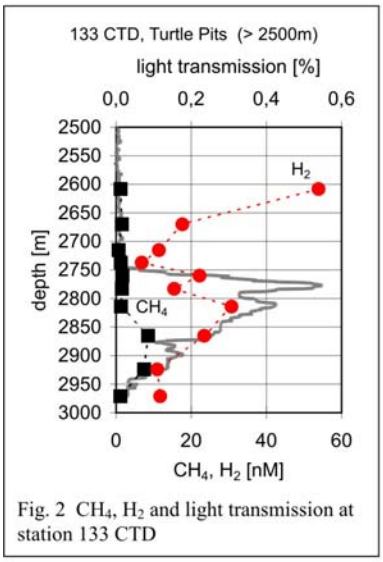

Fig. 2 CH_4, H_2 and light transmission at station 133 CTD

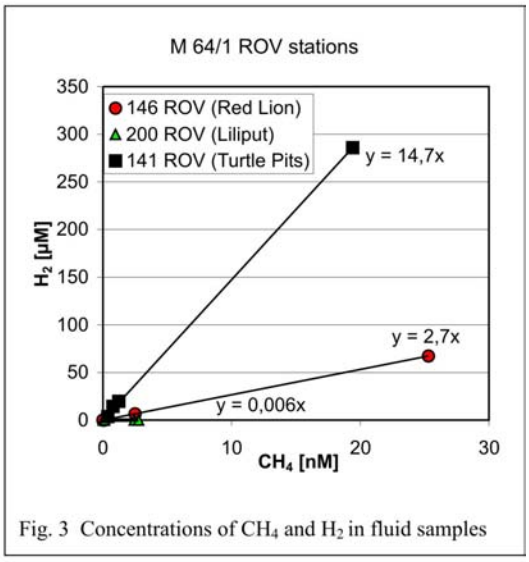

Fig. 3 Concentrations of CH_4 and H_2 in fluid samples

Work proceeded by prospecting for hydrothermal activity along the segment A3. Intense survey by CTD and gas measurement failed to recognise any hydrothermal imprint within the water column until station 186 CTD at 09° 27.03'S; 013° 13.99'W revealed considerably enhanced methane concentrations of up to 53 nmol L^{-1} (background < 1 nmol L^{-1}). Further investigation by numerous CTD casts allowed to presuming active hydrothermalism to occur within a relatively narrow area at about 1500m water depth. An extended area of diffusive fluid outflow accompanied by a dense population of mostly juvenile mussels was spotted and sampled during a ROV dive at this location, the Liliput hydrothermal field. This is by now the southernmost active hydrothermal area dicovered along the MAR. The emanating fluid was found to be H_2 prone but relatively rich in CH_4 (Fig. 3) with a H_2/CH_4 ratio of 0.006. The distribution of dissolved gases within the area indicates that the Liliput field does not considerably contribute to the observed anomalies but additional much stronger sources exist. However, no anomalies could be recognised within the CTD records, neither for light transmission nor for temperature. A second ROV attributed to searching for these sources had to be skipped for severe technical problems.

Table 1.2 CH_4 and H_2 concentrations found in MOR hydrothermal fluids. Note that all data refer to endmembers except those printed in bold (M64/1).

	H_2 [mmol L^{-1}]	**CH_4** [mmol L^{-1}]	**H_2/CH_4** molar ratio	ref.
Atlantic				
Peridotitic host rocks				
Rainbow 36°14‘N, MAR	13, 16	2,5	5.2-6.4	1, 2
Logachev 15°N, MAR	12	2.1	5.7	2, 13
Basaltic host rocks				
Broken Spur 29°N, MAR	0.43 – 1.03	0.07 – 0.13	6.6 – 7.9	3
Menez Gwen 37°17‘N, MAR	0.02 – 0.05	1.35 – 2.63	0.01 – 0.02	6
TAG 26°N, MAR	0.15 – 0.37	0.12 – 0.15	1.2 – 2.47	8, 2
MARK 23°N, MAR	0.19 – 0.48	0.02 – 0.06	7.7 – 8.3	10, 11
Lucky Strike 37°17‘N, MAR	0.02 – 0.07	0.0 – 0.97	0.03 – 0.07	8
Turtle Pits 04°49‘S, MAR	**0.29**	**0.02**	**14.7**	**14**
Red Lion 04°47‘ S, MAR	**0.08**	**0.03**	**2.87**	**14**
Liliput 09°33‘ S, MAR	**0.00002**	**0.003**	**0.006**	**14**
Pacific				
Endeavour. JdF, EPR	0.16 – 0.42	1.8 – 3.4	0.1 – 0.12	12
Southern JdF, EPR	0.27 – 0.53	0.08 – 0.12	3.3 – 4.5	9
21°N EPR	0.23 – 1.7	0.06 – 0.09	3.5 – 20	4
Galapagos	0.001 – 0.004	0.1 – 0.4	0.01 – 0.03	5

1: Donval et al., 1997; 2: Charlou et al., 2002; 3: James et al., 1995; 4: Welhan &Craig, 1979; 5: Lilley et al., 1983; 6: Charlou et al., 2000; 7: Kelley et al., 2001; 8: Charlou et al., 1996; 9: Evans et al., 1988; 10: Campbell et al., 1988; 11: Jean-Baptiste et al., 1991; 12: Butterfield et al., 1994; 13: own data M60/3; **14: This work**

For hydrocarbons of carbon chain lengths from 2 to 4 only saturated homologues were observed (ethane, propane, butanes), but in low concentrations. Molar ratios between methane and higher homologues (C_1/C_{2-4}) were generally above 2000.

1.4.6. Detection of hydrothermal plumes with backscatter MAPR system

(S. Fretzdorff, R. Seifert, C. Ostertag-Henning)

Introduction

The distribution of hydrothermal plumes within the studied areas has been determined with a Pacific Marine Environmental Laboratory (PMEL) Miniature Autonomous Plume Recorder (MAPR; (Baker and Milburn, 1997)) attached to the cabel of a rock-corer, CTD or TV-Grab. The MAPRs include a sensitve light backscatter sensor (LBSS) that provides a relative measure of particle concentration, a 0.001°C resolution thermistor and a strain gauge pressure sensor in a Ti pressure case. Power supply is warranted by four 9 V alkaline batteries. The sampling rate was usually 10sec during deployment, thus the MAPR recorded data approximately every 5 to 10m in the water column. During the first rock-corer stations the MAPR was attached 200m, and later about 80m above the equipment. During CTD stations 2 to 5 MAPRs were mounted 10, 20, 30m etc. above the CTD. In order to compare the signals of the different MAPRs and literature data, the backscattering intensity has been recalculated to nephelometric turbidity unity (NTUs) according to the expression

$$\Delta \text{ NTU} = (V_r - V_b)/a_n$$

where ΔNTU is the plume LBSS anomaly in excess of ambient water, V_r is the raw voltage reading of the LBSS, V_b is the background voltage not affected by hydrothermal plumes, and a_n is a factor unique to each LBSS determined from a laboratory calibration using formazine (Baker et al., 2001). All profiles recorded during individual stations of cruise M64/1 are shown in Figure 1.

Results

MAPRs were attached during 56 deployments of rock-corer, TV-Grab and CTD stations (Fig. 1.9). In the area of Turtle pits, Wideawake mussel field and Red Lion (4°47S to 4°48S) hydrothermal plume signals have been recorded in nearly all stations (Fig. 1.9a). Unfortunately, during the first TV-Grab and rock-corer stations the MAPR was mounted too high above the equipments to trace the complete plume signal (Fig. 1.9a). During the CDT stations and after mounting the MAPR only 80m above the rock-corer distinct plume peaks centered at approximately 200m above the seafloor could be recorded. The plume signals have a vertical extension in the water column between 150 to 200m (Fig. 1.9a). Only at rock-corer stations 119, 136, and 137 VSR there are no peaks in the recorded nephelometer profiles, probably due to the greater distances (up to 2 km) to the hydrothermal fields. The magnitudes of the anomaly vary from 0.01 up to 0.11 Δ NTU volts which is extremely high compared to other light backscattering peaks recorded in hydrothermaly active regions like e.g. along the East Pacific Rise (Baker et al., 2001).

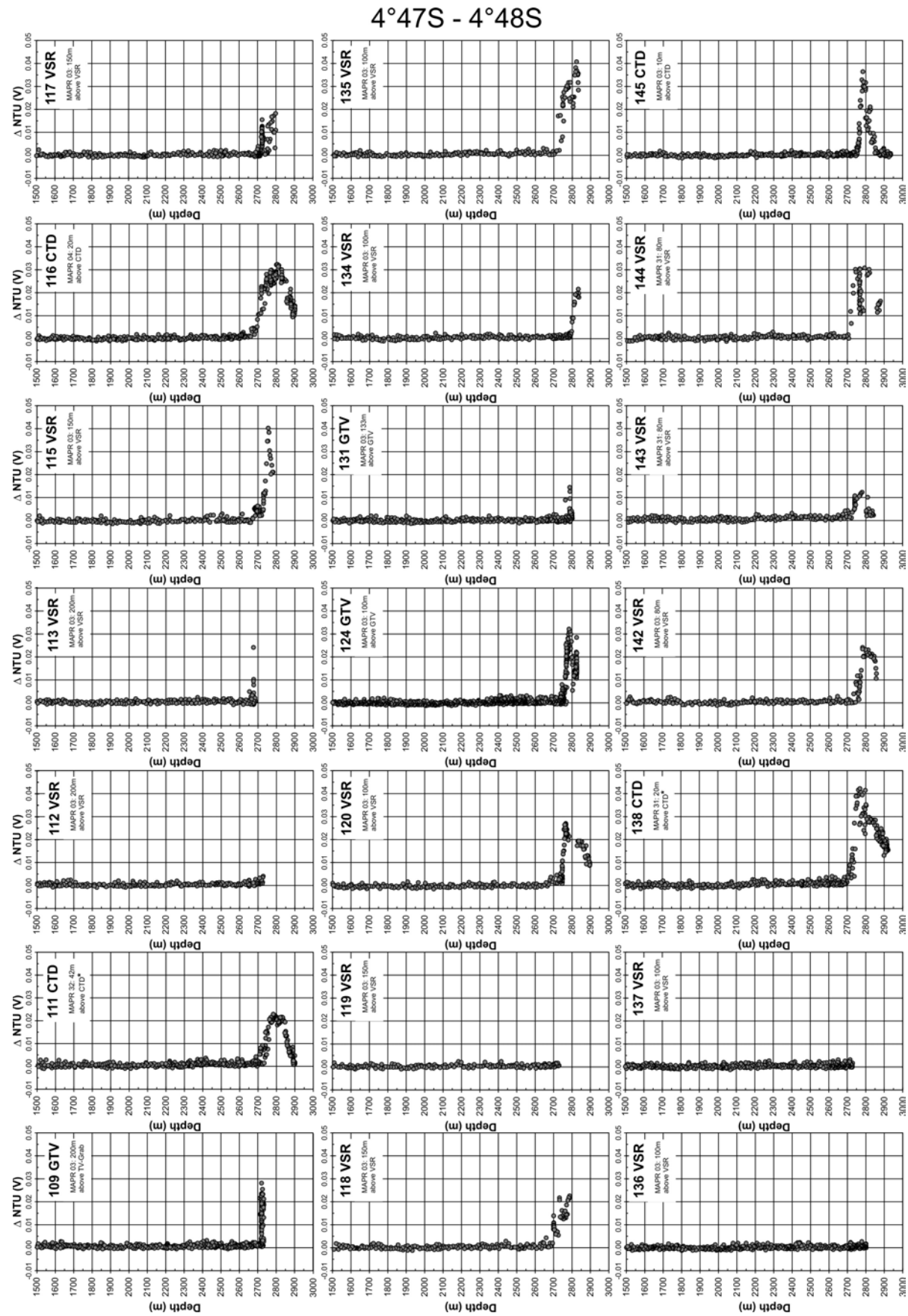

Figure 1.9a: Backscatter profiles (Δ NTU) from CTD and rock-corer stations in the area between 4°47 S - 4°48 S. *one example out of 3 MAPRs.

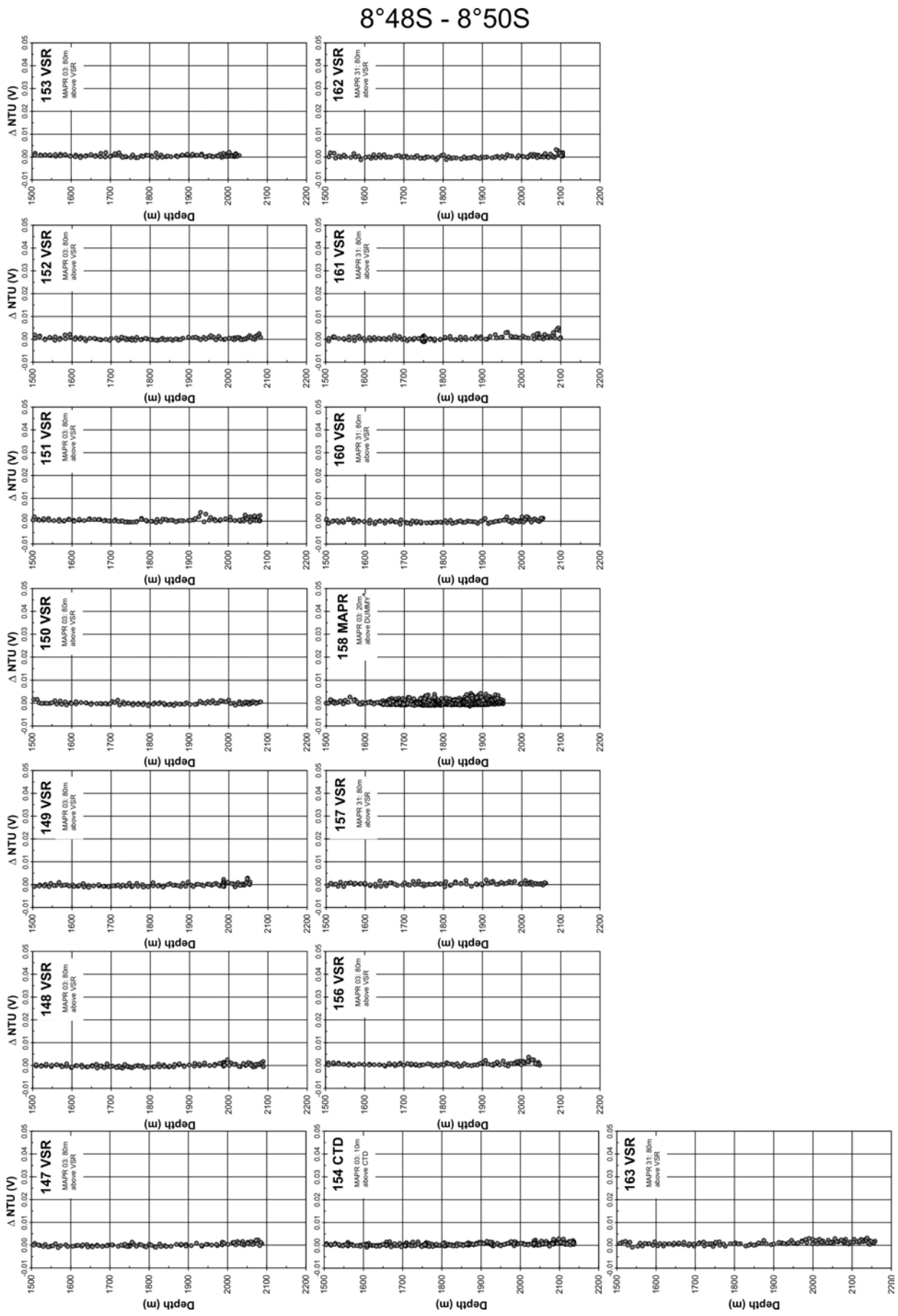

Figure 1.9b: Backscatter profiles (Δ NTU) from CTD and rock-corer stations in the area between 8°48 S - 8°50 S. *one example out of three MAPRs.

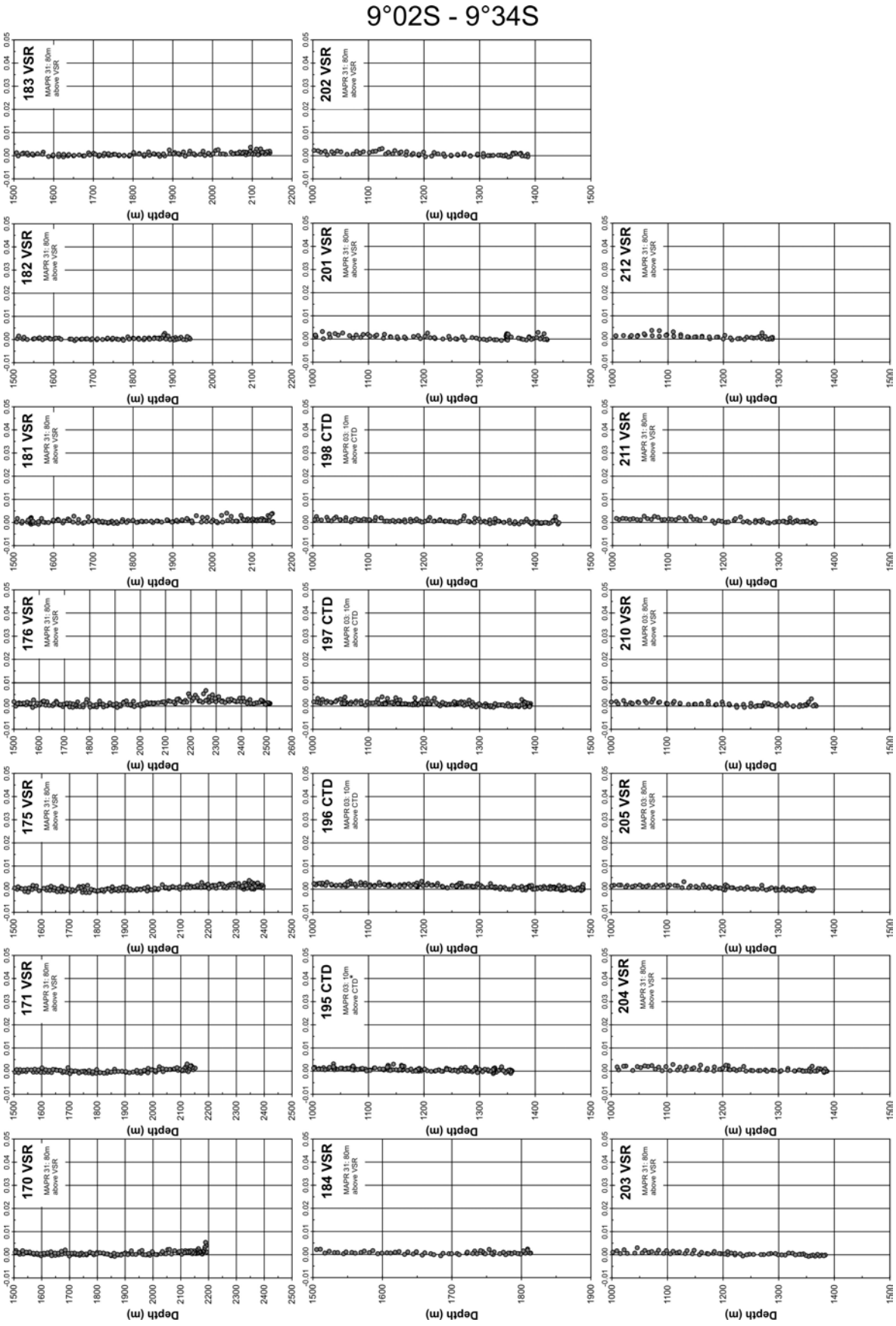

Figure 1.9c: Backscatter profiles (Δ NTU) from CTD and rock-corer stations in the area between 9°02 S - 9°34 S. *one example out of three MAPRs.

In order to map the distribution of the Turtle pits and Wideawake mussel field hydrothermal plumes five MAPRs were mounted 10m, 60m, 110m, 160m, and 210m above a DUMMY (several tyres) and were towed along 5 profiles. Temperature and light backscattering data have been collected during continuous lines of intersecting tow-yos in depth intervals of 2600 to 2900m. An exact x-y-z referencing of the recorded data was possible by using results from the GAPS transponder system. The data have been corrected and a three dimensional grid was constructed by using standard routines for gridding and interpolation in MATLAB onboard. The ΔNTU profiles show that the hydrothermal plumes above the Turtle pits and Wideawake mussel fields (located at 4° 48.6' S, 12° 22.36' W) are minor compared to a plume signal/source located west of the studied hydrothermal areas (Fig. 1.10). The output of the Turtle pits and Wideawake mussel field vents seems to be highly variable as evident from the discontinuous ΔNTU anomalies above these sites.

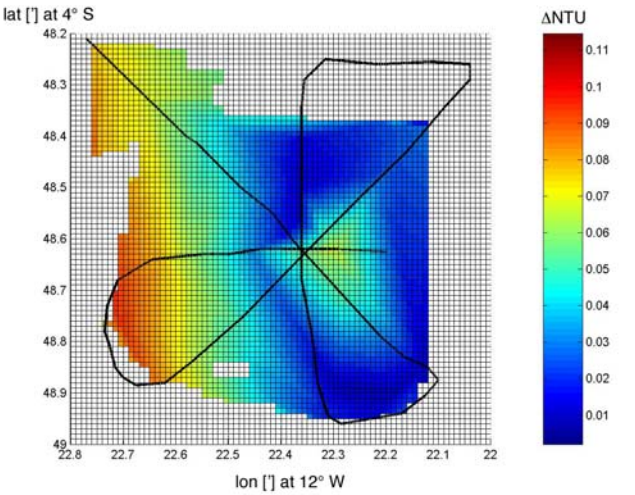

Figure 1.10a: Horizontal slice at 2830 m.

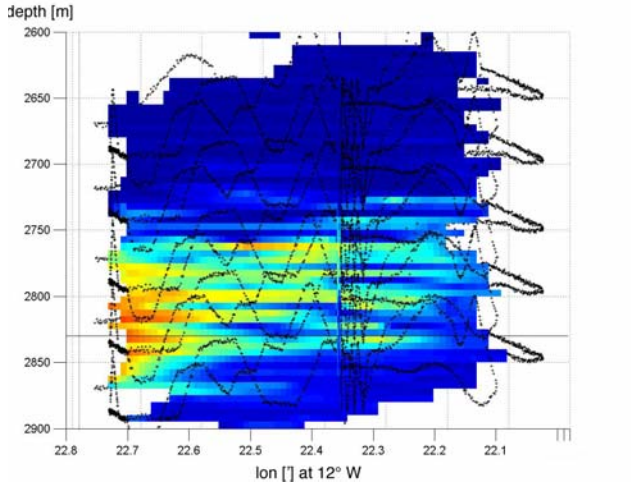

Figure 1.10b: Vertical slice at 4° 48.62' S.

In general, the recorded data in the area of Turtle pits, Wideawake mussel field and Red Lion show no sign of a temperature anomaly in the water column.

Further to the south, between 8°48S to 8°50S and 9°02S to 9°34S the light backscattering profiles show only straight lines, hence no signs of hydrothermal plumes in the water column even above the Lilliput vent field (Fig. 1.9b, c).

1.4.7. Zoology and Ecofaunistic Studies

(Jens Stecher, Olav Giere)

1.4.7.1. Goals

- to explore and sample the recently found hydrothermal habitats at 5°S.
- to describe their variability and compare the faunas with that of hydrothermal vents of the northern MAR.
- to select suitable vent locations for faunistic long-term-studies on benthic assemblages, to interpret spatial and time inhomogeneous structures of vent sites.
- to search for new hydrothermal habitats at 9°S

1.4.7.2. Methods

Observations were conducted via the ROV Quest (University of Bremen, Marum) and the Ocean Floor Observation System (OFOS, IFM-GEOMAR, Kiel). The ROV observations were made using a LWL-cable with three video cameras and a high-resolution digital still camera. The angle of observation was 84˚ with a maximum view of 15 m. The OFOS observations were made with a PAL black and white video camera, via coaxial cable. For detailed faunal mapping, a 35 mm analog still camera equipped with an underwater housing and water-corrected lens was used. Pictures were taken for detailed mapping every 30s. These still photographs will be processed after the cruise, and are thus not included in the preliminary results. The fauna was sampled mainly by two kinds of nets with meshes of 100µm and 300µm in diameter. These tools were handled by the manipulator arm of the ROV. In order to get an overview of the dominant taxa the TV-grab was used for sampling. The grab sampled an area of 2m². For meiobenthic analysis sediments were taken and completely preserved with 4% seawater-buffered formalin. Additionally, the shells of mussels and clams which were dissected for genetic analysis were preserved in pure 72% Ethanol. Within the first working area at 5°S samples were successfully taken at 9 of 13 stations. TV-grabs were only undertaken at Turtle Pits and Wideawake Mussel Field. At the Liliput hydrothermal field one dive with the ROV, two TV-graps and one OFOS station were driven (Table 1.3). The total bottom observation time at Turtle Pits was 31:44 [hh:mm], at Wideawake Mussel Field 10:20 [hh:mm], at Red Lion 18:24 [hh:mm], and at Liliput 15:35 [hh:mm] hours. With a total seafloor observation time of 76:03 [hh:mm] hours combined with successfully sampling at 13 stations, the following description of the faunal assemblages will give a representative first overview.

Table 1.3: List of stations of biological relevant surveys

Station/Tool	field / Location	Date/Bio samples (Yes/No)
108 ROV	Turtle Pits	08.04.2005 / No
114 ROV	Turtle Pits, samples taken at “Tower”	09.04.2005 / Yes
123 ROV	Turtle Pits , samples taken at “Tower”	11.04.2005 / Yes
125 ROV	Wideawake Mussel Field	12.04.2005 / Yes
130 ROV	Turtle Pits, sampled near marker M2	13.04.2005 / Yes
141 ROV	Turtle Pits	15.04.2005 / No
146 ROV	Red Lion, „Shrimps-Smoker“ sampled	16.04.2005 / Yes
200 ROV	Lilliput Hydrothermal field	25.04.2005 / Yes
109 GTV-A	Wideawake Mussel Field	08.04.2005 / Yes
110 GTV-A	Wideawake Mussel Field	09.04.2005 / No
124 GTV-A	Turtle Pits	11.04.2005 / No
131 GTV-A	Turtle Pits, nearby „Stalagmite“	13.04.2005 / Yes
132 GTV-A	Wideawake Mussel Field	13.04.2005 / Yes
139 GTV-A	Turtle Pits, sediments between sulphides	14.04.2005 / Yes
213 GTV-A	Liliput Hydrothermal field	27.04.2005 / Yes
214 GTV-A	Liliput Hydrothermal field	27.04.2005 / Yes
215 OFOS	Liliput Hydrothermal field	27.04.2005 / Yes

1.4.7.3. The vent site at 5°S

This site consists of three active hydrothermal habitats. The dominant taxa are decapode crustaceans such as Alvinocarididae, Mirocarididae, and Bythograeidae as well as mussels of the genus *Bathymodiolus*. Within the Wideawake Mussel field the grab samples showed that limpets and annelids are widely distributed, too. Additionally, sea anemones and scyphozoa occur in the different habitats. Besides these general structures each habitat shows own faunistic characteristics.

Decapoda

Generally, only *Rimicaris* and *Mirocaris* were found and no *Chorocaris* and *Alvinocaris* were observed. At the smokers of Turtle Pits, both species were sampled at two different smokers with *Rimicaris* being dominant. This stands in contrast to the distribution patterns in the Wideawake Mussel Field. There we sampled more *Mirocaris* than *Rimicaris*, it seemed to be that here *Mirocaris* is more abundant than *Rimicaris*.

At the Red Lion field, consisting of four active black smokers we found only *Rimicaris* in large abundance. At least two smokers, “Shrimps Smoker” and “Sugar Head”, were covered by *Rimicaris* in such dense populations, that the chimneys appeared white. These *Rimicaris* were quite abundant and wide distributed in the vicinity of the field at pillow lava structures, up to 20 m away from the active smokers tending north.

The brachyurian crab likely is *Segonzacia mesatlantica*. It was collected at the chimneys of Turtle Pits and among *Bathymodiolus* specimen at Widewake Mussel Field. They are further abundant at the active chimneys of Red Lion.

Fig. 1.11: Decapod crustacean on the “Tower” of Turtle Pits. Specimens of *Rimicaris* c.f. *exoculata*, *Mirocaris*, and *Segonzacia* c.f. *mesatlantica*.

Bivalvia and Gastropoda

At Turtle Pits no dense patches of living Bathymodiolus were found. Only at the margins of the pits as well on the flanks we found some rare specimen. Most of them were dead like at the bottom of active smokers where only shells of dead Bathymodiolus could be seen. Neither snails like *Phymorhynchus* nor limpets were present.

In contrast, at the Wideawake Mussel Field living specimens dominated clearly over the dead ones. Within two TV- grabs (each of them covering about 2m²) more than 250 living specimen of Bathymodiolus were retrieved and no dead shells were among these samples. Additionally only few scavengers like *Phymorhynchus* were documented.

This picture changed in the southern part of the field. Here vesicomyid clams were found interspersed in *Bathymodiolus* beds. Although several of the vesicomyid clams were still alive, many of them were dead and not longer than 12 cm. Stecher et al. (2002) discussed the change of a natural ageing cycle of diffuse hydrothermal venting, in which clams were replaced by mussels. So a shift of the hydrothermal activity seemed to be visible here in the community structure, which were based on symbiontic microorganisms. Additionally, the scavenger *Phymorhynchus* was more abundant.

Remarkable were the different distribution patterns of limpets: Whereas limpets settled mostly on basalts within the central Wideawake Mussel Field, which is built of single patches of Bathymodiolus linked by bands of mussels, they were living on the shells of Bathymodiolus in the north-western periphery of the field. The mussels were obviously more patched than within the centre.

With only one exception we did not find any bivalves as well as gastropods at the active smokers of the Red Lion Field. In the northern part of the field we found no more than 60 specimens sitting near the bottom off an inactive smoker. This part of the massive sulphide block was coated by a small white band. If this band consists of bacteria, this might be a sign of slight hydrothermal activity.

Fig. 1.12: The *Bathymodiolus* – vesicomyid clam association in the southern part of Wideawake Mussel Field.

Annelids

We identified at least six forms: Terebellida (forms like Ampharetinae), Chaetopterida, some Phyllodocidae (Polynoidae, Spionida), Malanidae, and Archinomidae. These were all sampled in Wideawake Mussel Field mostly within the byssus filaments of Bathymodiolus. Only the spionids were attached with their tubes on basalt.

Cnidaria

Especially in the Wideawake Mussel Field small anemones and scyphozoa settled in dense aggregations on basalt blocks. Larger specimen of sea anemones were regularly observed on the active smokers of Turtle Pits as well as in between the *Bathymodiolus* patches of the Wideawake Field.

1.4.7.4. The vent site at 9°33'S – Liliput

The Liliput hydrothermal field is characterised by pillows which are coated with Fe- oxides so that the field appeared in red-orange colours. Shimmering water emerged out of cavities between pillow lavas. Young specimen of *Bathymodiolus* occurred in dense elongated populations along the cavities and along the pillow's cracks. Obviously, postlarval young mussels (0.5mm length) had settled this vent field recently whereas shells of adults were dissolved. Only their periostracum was found with juveniles attached to them by their byssus filaments. The only undissolved shells were found where no active ventig was observed. Their length did not exceed 12cm. Shrimps and bythograeid crabs were subdominant, only a few specimen were observed directly at the source of shimmering water. Additionally, scavengers like Phymorhynchus were seen in the periphery. Grazers like limpets were not observed. In the vicinity of the mussel beds single gorgonians were sitting on the Fe-oxides coated pillows. These morphotypes of gorgonians are characteristic species of the hydrothermal periphery. These facts indicate that this site is a reactivated diffuse venting site which was recently settled by a new generation of mussels.

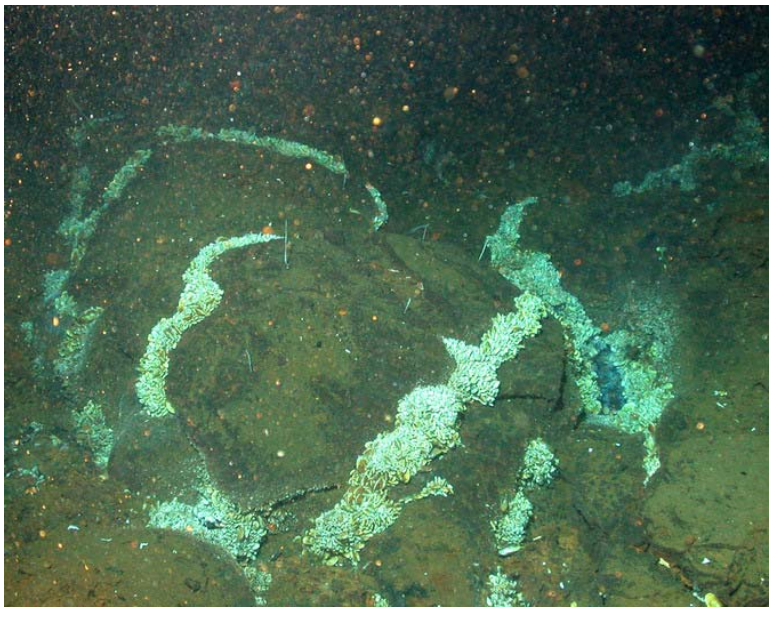

Fig. 1.13: The Bathymodiolus association at Liliput.

Conclusions:

The identified taxa of the hydrothermal fields at 5°S and 9°33´S on the Mid-Atlantic Ridge resemble the northern Logatchev community (Gebruk et al. 2000) in most elements. Remarkable is the missing of following typical hydrothermal taxa within the new discovered fields:

Decapods of the families Alvinocaridae, like *Alvinocaris* and *Chorocaris*, and Galatheidae, echinoderms like Ophiuridae and Ventfishes of the family Zoarcidae.

Obviously, the St. Pauls and Romanche Fracture Zones act only partly as a physical barrier between vent fauna assemblages of the North and South Atlantic Oceans (see Shank 2004).

Therefore, the spatial environmental conditions seemed to be more responsible for faunal differences rather than geographic isolation mechanisms. This stands in line with the results of Desbruyères et al. (2001), comparing different vent fields an the northern Mid-Altlanic Ridge. Therefore they suggested that future investigations should be focused on time series concerning the inter- and intraspecific competitions as well as the variability of microenvironments along gradients.

1.4.8. Molecular and structural analysis of symbioses

(Olav Giere)

Our studies followed several investigative lines:

- Molecular comparison of host tissue and symbiotic bacteria from various vents: Do the newly discovered vents south of the MAR fracture zone conform with those from the Logatchev vent field. Are there differences that could relate to a biogeographic separation? Host animals: *Bathymodiolus* cf. *puteoserpentis* (vent mussels) and *Rimicaris exoculata* (vent shrimps).
- Molecular analysis of genetic changes in both host and bacteria from various vent fields: is there a co-evolution between the symbiotic partners or do they evolve independently (cooperation with T. Shank, Woods Hole)?
- Molecular and ultrastructural comparison of the endobacterial consortium harboured in *Bathymodiolus* cf. *puteoserpentis*: does the relation of methanotrophic to thiotrophic bacteria vary at the different vent fields, possibly depending on the varying concentrations of methane and hydrogen sulphide (link to results from projects analysing the fluid chemistry)?
- Analysis of the establishment of the symbiosis: At what stage do the mussel hosts acquire their symbionts from the environment, i.e. contain the newly settled mussels (size 1 – 2 mm) already the complete set of bacteria? Is their distribution in the bacteriocysts identical to that in adult hosts (FISH and ultrastructural studies)?

The material retrieved at both vent fields sampled (4^{o}48 S and 9^{o}33 S) allows for answering all the different approaches outlined above. Results are to be expected after careful analyses in the home labs.

4^{o}48 S: From Wideawake Mussel Field all size ranges of *Bathymodiolus* c.f. *puteoserpentis* could be dissected and the parts fixed; even newly settled specimens in the mm-size class were retrieved. The new hot vent "Shrimp Smoker" yielded numerous *Rimicaris exoculata* of various size classes. The few specimens of Mirocaris fortunata sampled allow for the first molecular analysis of possible ectosymbionts on the mouth parts. In addition two specimens of *Calyptogena* sp. were sampled at another, yet unnamed hot smoker, and dissected for molecular analysis. This will enable us to analyse for the first time molecular biologically the symbiosis of an Atlantic species of *Calyptogena.*

9^{o}33 S: Again *Bathymodiolus* c.f. *puteoserpentis* of all size classes

Some limpets populating preferably the mussel shells at Wideawake Mussel Field have been fixed for an exploratory molecular and ultrastructural inspection for symbiotic bacteria (in the gills?).

Compilation of material retrieved:

4^{o}48 S: *Bathymodiolus* c.f. *puteoserpentis*: 30 specimens

Rimicaris exoculata: 46

Mirocaris fortunata: 8

Calyptogena sp.: 2

Limpets: 21

9°33 S: *Bathymodiolus* c.f. *puteoserpentis*: 50 specimens, from newly settled to juvenile; not all sizes allowed for dissection

1.4.9. Microbiology

1.4.9.1. Samples and methods

Basalts

(C. Flies)

During the cruise M64/1 different basaltic rocks should be collected

a) to determine the microbial diversity in cracks and pores of basaltic rocks of different age (started on board continued in the home laboratory). This will be done by several cultivation experiments to isolate aerobic/anaerobic, organo-/lithotrophic and/or heterotrophic/autotrophic microorganisms.
b) to investigate the microbial diversity of the samples in the home laboratory by molecular analysis like clone libraries of 16S rRNA genes (*Archaea* and *Bacteria*) in combination with amplified ribosomal rDNA restriction analysis – ARDRA and denaturing gradient gel electrophoresis – DGGE.
c) to study the community structure and morphology of *Bacteria* and *Archaea* in the basaltic rock by electron microscopy and fluorescence in situ hybridization – FISH
d) to calculate the microbial occurrence and abundance in basaltic rocks based on several geochemical techniques (extraction of organic substances and analysis of specific biomarkers including isotopic analysis) in the home laboratory. Geochemical methods should also be used to analyze pure cultures to correlate the obtained data with single species or specific groups.
e) to determine sulfate and secondary mineralization products (iron and manganese) by anorganic extraction methods and isotopic analysis in the home laboratory. This products will also be analyzed by FTIR and powder-XRD. Furthermore, the correlation between the biological colonization and the precipitation of secondary minerals should be investigated.

To combine the results for a better understanding of the interactions between basaltic rocks and microbial activity all investigations will be done on identical samples.

Furthermore samples from sediment, deep sea water and surface water should be investigated by microbiological and molecular analysis to get the information about the microbial diversity outside basaltic rocks.

Hydrothermal systems - fluids, sediments and mineral phases

(J. Süling, M. Perner, J. Küver)

The aim of the cruise was the collection of material in order to perform

a) Molecular analyses of the microbial community structure of hydrothermal vent systems at 4°48 S and 9°33 S in comparison to the Logatchev vent field (in the home lab)
   - Construction of clone libraries using the 16S rRNA gene (Archaea and Bacteria); Qualitative analyses of present microorganisms.
   - 16S rRNA gene targeted DGGE (Archaea and Bacteria).
   - FISH (Fluorescence in situ Hybridization); Quantification of major phylogenetic groups.
   - Functional gene analyses based on *soxB* (sulfide oxidation), *aprAB* (sulfate reduction, sulfide oxidation), key enzymes of the reductive TCA- cycle, and other CO_2-fixation pathways.
b) Cultivation based experiments using specific media (started on board and continued in the home lab)
   - Selective media for autotrophic microorganisms using various electron donors (H_2, H_2S, S°, S_2O_3, Fe^{2+}, CH_4) as well as suitable electron acceptors (O_2, NO_3, Fe^{3+}, Mn^{4+}, S°, S_2O_3) in the presence of CO_2.
   - Selective media for aerobic and anaerobic heterotrophic microorganisms.
c) On board microscopic observations of microorganisms inhabiting freshly taken samples.

1.4.9.2. Results

Basalts

Basaltic rocks from different locations and different ages were taken using the TV grab or ROV (detailed informations will be present in the extended version of the cruise report). The samples were transferred into an anaerobic chamber which was filled with nitrogen. Macroscopic visible organisms like Actiniaria were collected and fixed with ethanol or other fixatives and stored at 4°C or at room temperature. The rock surfaces were sterilized with ethanol and the rock was broken in several pieces using a sterilized hammer and a chisel. Most of the pieces were stored at -20°C, air dried or fixed with glutardialdehyde and formaldehyde for further molecular and geochemical analyses in the home laboratory. Other fragments were separated on bord in different subsamples (crust, glass or basalt) and each zone was crushed with a sterile mortar. The splints were used for aerobic and anaerobic cultivation. For aerobic plates the splints were “suspended” in sterile seawater and this solution was used as inoculum. The cultures were incubated at room temperature and transferred to 4°C after several days. In the home laboratory further experiments will be done e. g. agar shakes to obtain pure cultures. Additionally both, splints and the “suspended” basalt were used as inocula for permanent cultures which were stored at -20°C.

Sediment and water samples:

Sediment samples as well as water samples from the deep sea taken by CTD and surface water were used for permanent cultures and aliquots were frozen for molecular analysis for further investigations in the home laboratory. On bord several cultivation experiments were carried out.

Hydrothermal systems - fluids, sediments and mineral phases

a) Molecular analyses of the microbial community structure of hydrothermal vent systems will be conducted in the home lab. Samples were taken via the fluid sampling system from diffusive vents as well as from fluids of black smokers during ROV cruises. Other samples represent hydrothermally influenced rocks and sediments which were retrieved via the TV-grab and the wax corer. The samples were frozen at -20°C and fixed for further treatment. Plume samples were taken using the CTD. These samples were filtered and immediately frozen at -20°C or fixed for further processing. Detailed information on single samples is shown in the extended version of the cruise report for each working group.

b) The samples mentioned above were also used for obtaining enrichment cultures. For this purpose selective media as indicated above were used. Growth was monitored by microscopic observation. Autotrophic as well as heterotrophic microorganisms in culture include various morphotypes. Further processing will be conducted in the home lab with the aim to obtain pure cultures.

c) Microscopic observations of microorganisms inhabiting freshly taken samples revealed heterogenous morphotypes in most samples. Interestingly enough on rock samples collected by the 132 TV-grab at the boarder of a *Bathymodiolus* sp. dominated mussle field two very obvious morphotypes containing sulfur globuli were observed. The white structures (0.5-2mm length) seen in Figure 1.14 consist of several filaments resembling the typical morphological features of *Thiotrix* sp. (non gliding, rosette formation and modified base cells for the attachment to hard substrates). The entire rock sample was irregularly covered by these structures. The filaments enclosed high numbers of sulfur globuli and had a width of up to 20µm.

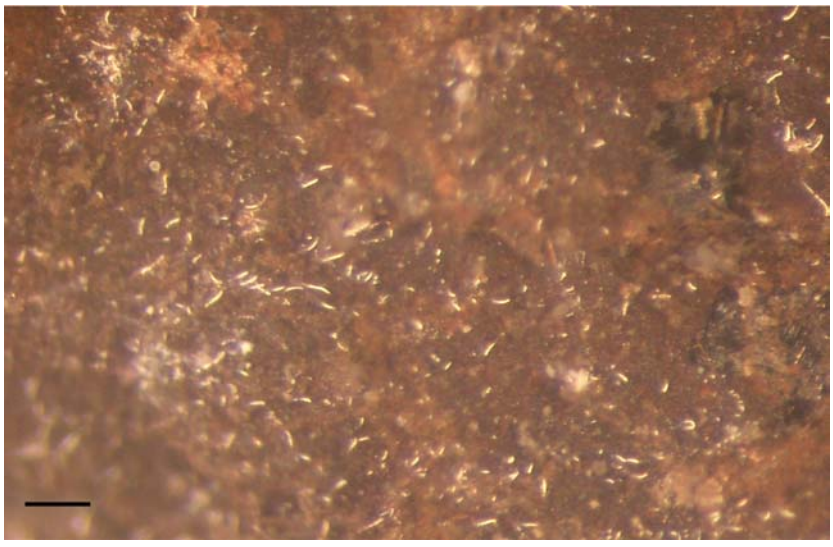

Fig. 1.14: Surface of a rock sample recovered by the 132 TV-grab. The white structures resemble *Thiotrix sp*. Scale bar 2mm. Photo by H. Paulick.

In addition to the sample mentioned above, a sample from 109 TV-grab also collected within the vicinity of a mussel field exhibited a coccoid organism containing numerous sulfur globuli with obvious similarity to *Achromatium* spp. (Fig. 1.15). Besides this large colourless sulfur bacterium which is non motile, several other highly motile small rods and vibrios were observed.

To our knowledge this is the first observation of these two microorganisms at deep sea hydrothermal vent systems. *Thiotrix* spp. have only been found in marine influenced cave systems and like *Achromatium* spp. are known from shallow water hydrothermal vent systems like the golf of Napoli or Paleochori Bay (Milos island).

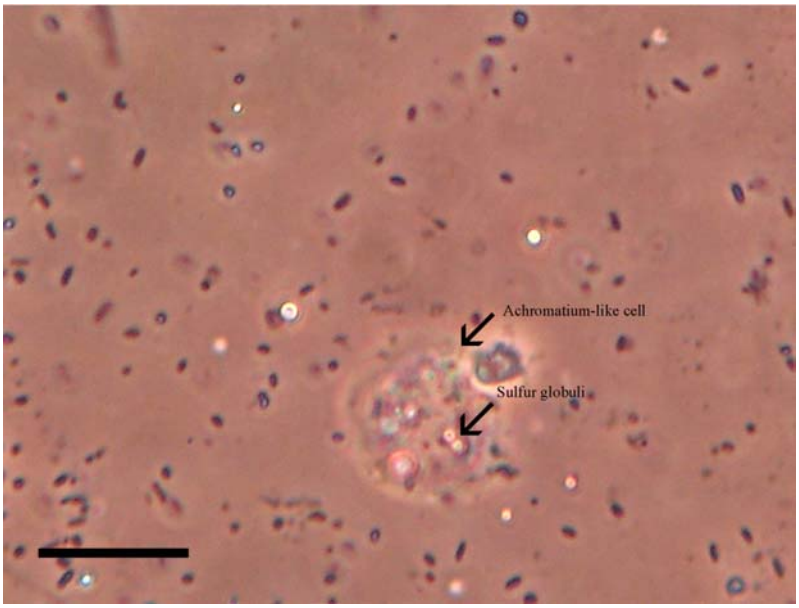

Fig. 1.15: Microscopic picture from an Achromatium-like organism (diameter 20µm) with enclosed sulfur globuli. Scale bar 20µm. Photo by H. Paulick.

1.4.10. QUEST Deepwater ROV

(V. Ratmeyer, A. Houk, S. Klar, P. Mason, N. Nowald, W. Schmidt, M. Schroeder, C. Seiter)

The deepwater ROV (remotely operated vehicle) "QUEST 4000m" used during M64-1, is operated by and installed at MARUM, Center for Marine Environmental Sciences at the University of Bremen, Germany. The QUEST is a commercially available, specially adapted for marine science, and 4000 m rated system designed and build by Schilling Robotics, Davis, USA. Aboard RV METEOR for the 5th cruise since installation in Mai 2003, the system is well adapted to the research vessel and could be handled during all stages of weather encountered during the cruise.
During M64-1, QUEST performed a total of 13 dives between depths of 1400 and 3100 m. 12 dives with al total of 98 hours bottom time allowed successful scientific sampling and observation at different sites along the Mid Atlantic Ridge.

The total QUEST system weighs 45 tons (including the vehicle, control van, workshop van, electric winch, 5000-m umbilical, and transportation vans) and can be transported in four 20-foot

vans. Using a MacArtney Cormac electric driven storage winch to manage the 5000m of 17.6 mm NSW umbilical, no additional hydraulic connections are necessary to host the system.

The QUEST uses a Doppler velocity log (DVL, 1200kHz) to perform Stationkeep, Displacement, and other auto control functions. Designed and operated as a free-flying vehicle, QUEST system exerts such precise control over the electric propulsion system that the vehicle maintained positioning accuracy within centimeters and decimeters. In addition, absolute GPS positions are obtained using self-calibrating, acoustic IXSEA GAPS USBL positioning system. However, performance of the system was limited to an absolute accuracy below 20 m. For future cruises, absolute position accuracy will hopefully be substantially enhanced after a major upgrade of the GAPS acoustic array.

The combination of 60-kW power with DVL -based auto control functions provides exceptional positioning capabilities at depth. During many dives, QUEST was able to hold position at various depths between 1400 and 3100 m against all currents and cable movements. During dives at the hydrothermal vent fields, the DVL-based, automatically controlled 3D positioning capability allowed highly precise operations for close-up video filming and up to 1 hour continuous fluid sampling on vertical vent structures without vehicle seafloor contact.

The QUEST SeaNet telemetry and power system provides an extremely convenient way to interface all types of scientific equipment, with a current total capacity of 16 video channels and 60 RS-232 data channels. The SeaNet connector design allows easy interface to third-party equipment, particularly to prototype sensor and sampling devices, by combining power-, data-, video-distribution plus compensation fluid transport all through one single cable-connector setup . This ease of connection is especially important in scientific applications, where equipment suites and sensors must be quickly changed between dives. When devices are exchanged, existing cables can be kept in place, and are simply mapped to the new devices, which can consist of video, data, or power transmission equipment.

The substantial empty space inside the QUEST 5 frame allowes installation of mission-specific marine science tools and sensors. The initial vehicle setup includes two manipulators (7-function and 5-function), five video cameras, a digital still camera (SCORPIO, 3.3 Megapixel), a light suite (with various high-intensity discharge lights, HMI lights, lasers, and dimmable incandescent lights), a CTD, a tool skid with drawboxes, an acoustic beacon finder and a 675 kHz scanning sonar. Total lighting power is 5 kW, and additional auxiliary power capacity is 8 kW.

During M64-1, additional scientific equipment was installed:

- fluid pump system with remote sampling and temperature probe
- microbiological filtering system
- various “hand” tools including nets, scoops, markers, and an autonomous fluid sampler

For detailed video closeup filming, a near-bottom mounted broadcast quality (870 TVL) 3CCD video camera was used (ATLAS). Continuous video footage was recorded with the ATLAS camera and one additional color zoom video camera (PEGASUS or DSPL Seacam 6500). In order to gain a fast overview of the dive without the need of watching hours of video, one video feed is continuously frame-grabbed and digitized at 5sec intervals.

The QUEST control system provides transparent access to all RS-232 data and video channels. The scientific data system used at MARUM feeds all ROV- and ship-based science and logging channels into a commercial, adapted real-time database system (DAVIS-ROV).
During operation, data and video are distributed in realtime to minimize crowding in the control van. Using the existing ship's communications network, sensor data is distributed by the real-time database via TCP/IP from the control van into various client laboratories, regardless of the original raw-data format and hardware interface. This allows topside processing equipment to perform data interpretation and sensor control from any location on the host ship.

Additionally, the pilot's eight-channel video display is distributed to client stations in labs and bridge on the ship via CAT5 cable. This allows the simple setup of detailed, direct communication between the bridge and the ROV control van. Similarly, information from the pilot's display is distributed to a large number of scientists. During scientific dives where observed phenomena are often unpredictable, having scientists witness a "virtual dive" from a laboratory rather than from a crowded control van allows an efficient combination of scientific observation and vehicle control.

Post-cruise data archival will be hosted by the information system PANGAEA at the World Data Center for Marine Environmental Sciences (WDC-MARE), which is operated on a long-term base by MARUM and the Foundation Alfred Wegener Institute for Polar and Marine Research, Bremerhaven (AWI).

1.5. Weather Conditions during M64/1

(W. Ochsenhirt)

On April 02 forenoon MV METEOR left the port of Mindelo (Cape Verde Islands) heading south. The winds encountered were constant northeasterly tradewinds of Bft 4 or 5. On April 06 the reasearch vessel came to the intertropical convergence zone (ITCZ) near 8°N. When Passing the ITCZ the winds were calm and variable and during the following night an intensive tropical shower occured. On the next day near 02.30 North the ITCZ was already far north of the ships position. The Equator was crossed in the afternoon of April 06 and the tradewinds came from southeast with Bft 4 or 5.

In the evening of April 07 the first investigations started near 4.48°S, 12.24°W and were continued until 09.43°S, 13.06°W. During this time METEOR was situated at the edge of the subtropical high in the central South Atlantic. The southeasterly tradewind was mostly steady with 4 or 5, Bft, only for short periods Bft 6. Swell from south or southeast often occurred with a height of 2, sometimes up to 3 m.

In the afternoon of April 27 the investigations ended and METEOR headed for Fortaleza in a direct course. Under the influence of southeasterly to easterly following tradewinds of 3 to 5 Bft the transit voyage was no problem. METEOR arrived in Fortaleza in the early morning of May 03.

1.6. Station List M64/1

Station	Date	Lat. (S)	Long. (W)	Depth (m)	Rock description
109GTV-1	08.04.2005	04°48.64	12°22.36	2998	Fresh, glassy basalt; aphyric sheet flow.
109GTV-2	08.04.2005	04°48.64	12°22.36	2998	Very fresh aphyric sheet flow, wrinkled surface.
109GTV-3	08.04.2005	04°48.64	12°22.36	2998	basalt with 1 cm glass crust.
109GTV-4	08.04.2005	04°48.64	12°22.36	2998	Piece of fresh, glassy sheet flow lava, wrinkled surface, aphyric.
109GTV-5	08.04.2005	04°48.64	12°22.36	2998	Fresh, aphyric sheet lava with 1 cm glass rind on both sides.
110GTV-1	09.04.2005	04°48.55	12°22.36	2998	Fresh, aphyric sheet flow, 1 cm glassy rim.
110GTV-2	09.04.2005	04°48.55	12°22.36	2998	Aphyric basalt glass.
110GTV-3	09.04.2005	04°48.55	12°22.36	2998	Fresh aphyric basalt, glassy margins on both sides of sample.
111CTD	09.04.2005	04°48.6	12°22.4	2998	
112VSR-1	09.04.2005	04°48.75	12°22.28	2995	Small glass particles.
113VSR-1	09.04.2005	04°48.77	12°21.76	2951	Fresh, aphyric basalt glass.
113VSR-2	09.04.2005	04°48.77	12°21.76	2951	Fresh glassy ash with foram. sand.
114ROV-4A*	10.04.2005	04°48.579	12°22.418	2993	Piece of black smoker chimney, zoned, interior consists of chalcopyrite (friable, porous). Outer rim: 1-2 cm of pyrite-marcasite, marcasite-rich outer crust coated with Fe-Oxihydroxides.
114ROV-5A*	10.04.2005	04°48.579	12°22.418	2993	Zoned black smoker chimney. Outer 2 - 5 cm: pyrite-marcasite crust, interior; chalcopyrite-rich with abundant anhydrite and rare sphalerite. Prominent ribbon banding. Central conduit is open: 4 to 9 cm in diameter lined and filled by anhydrite (partially intergrown with fine- grained sulfide [sphalerite?]).
114ROV-5B-F*	10.04.2005	04°48.579	12°22.418	2993	Several small pieces of pyrite-marcasite black smoker crustal material, behive-like layering.
114ROV-5G-H*	10.04.2005	04°48.579	12°22.418	2993	Porous, friable chalcopyrite-rich material from black smoker interior.
114ROV-5Bag*	10.04.2005	04°48.579	12°22.418	2993	Loose sulfide rubble, very porous, soft, collected in bionet.
114ROV-6*	10.04.2005	04°48.579	12°22.418	2984	Sample of beehive structure, similar to sample 114-4; outer marcasite crust, interior is porous chalcopyrite showing behive layering.
114ROV-7*	10.04.2005	04°48.579	12°22.418	2984	Piece adjacent to 114-6 but not behive structured (more like a layered knob); marcasite-rich outer crust; chalcopyrite-rich interior.
115VSR-1	10.04.2005	04°48.77	12°22.61	3048	Basalt glass with large plagioclase phenocryst (10 mm in diameter).
115VSR-2	10.04.2005	04°48.77	12°22.61	3048	Glass particles with plagioclase phenocrysts.
116CTD	10.04.2005	04°48.8	12°22.7	2961	
117VSR-1	10.04.2005	04°48.25	12°23	3033	Two small pieces of aphyric basalt glass.
118VSR-1	10.04.2005	04°48.26	12°22.23	3000	Very fresh aphyric glass.
119VSR-1	10.04.2005	04°48.26	12°21.48	2980	Fresh basaltic glass with plagioclase phenocrysts (max. 1 cm).
120VSR-1	10.04.2005	04°47.79	12°22.97	3050	~1 cm thick glass crust, basalt with several plagioclase phenocrysts up to 1 cm.
121CTD	11.04.2005	04°47.8	12°22.6	3022	
122CTD	11.04.2005	04°48.5	12°22.4	2971	

Station	Date	Lat. (S)	Long. (W)	Depth (m)	Rock description
123ROV-4A*	11.04.2005	04°48.583	12°22.41	2986	Outer portion of active chimney consisting of numerous, friable microchimney structures (1 - 5 cm diameter). Marcasite crust. Interior is complex and zoned grading from anhydrite, sphalerite to pyrite-sphalerite to chalcopyrite. Exterior is partially oxidized and locally covered with white bacterial? dots.
123ROV-4B*	11.04.2005	04°48.583	12°22.41	2986	Two fragments of chimney interior, chalcopyrite-anhyydrite association.
123ROV-4C*	11.04.2005	04°48.583	12°22.41	2986	Various fragments of chimney exterior, marcasite-pyrite + Fe-oxihydroxide + white coatings. Finer rubble with chalcopyrite-rich material, anhydrite, microchimneys.
123ROV-8	11.04.2005	04°48.58	12°22.4	2985	Aphyric basalt, lobate feature on surface of jumbled sheet flow. 3 mm thick glass on both sides. Interior is microcrystalline with large lensoidal cavities parallel to outer surfaces (drain-out feature?) lines with thin Mn-Oxide film.
123ROV-9*	11.04.2005	04°48.559	12°22.413	2990	Piece of inactive sulfide chimney, recrystallized. Chalcopyrite-rich interior ca. 5 cm in diameter, partly oxidized (pigeon coloration). Outer zone is sphalerite-pyrite-marcasite. Crust is marcasite, outer crust is 1 mm thick Fe-oxihydroxide.
124GTV-1A*	11.04.2005	04°48.573	12°22.424	2998	Three pieces of approx. similar size, slabby blocks of aphyric basalt, 1-2 mm of glass crust on both sides and extensive Fe-oxihydroxide coating.
124GTV-1B*	11.04.2005	04°48.573	12°22.424	2998	Similar to 124-1A but with prominent wrinkles on the surfaces.
124GTV-2A*	11.04.2005	04°48.573	12°22.424	2998	Massive pyrite/marcasite; outer 5 mm biogenic(?) marcasite crust followed by 1 cm massive marcasite, interior pyrite: dendritic growth cross cutting beehive layering.
124GTV-2B*	11.04.2005	04°48.573	12°22.424	2998	Same as 2A + small normal fractures lined with chalcopyrite. Zones of sphalerite enrichment.
124GTV-2C*	11.04.2005	04°48.573	12°22.424	2998	Same as 2A but interior is with more chalcopyrite (Cu-rich end member of this type).
124GTV-2 D to M*	11.04.2005	04°48.573	12°22.424	2998	Crustal material of black smoker chimney: pyrite + marcasite, rare to trace sphalerite + chalcopyrite in cavities and along fractures.
124GTV-2G*	11.04.2005	04°48.573	12°22.424	2998	Similar to 2A but more black sphalerite, Zn-rich end member of this type.
124GTV-3 A to -C*	11.04.2005	04°48.573	12°22.424	2998	Massive pyrite-marcasite with strong beehive texture.
125ROV-1A	12.04.2005	04°48.6111	12°22.327	3000	Glassy aphyric lava with large vesicle (max. diameter is 5 cm) and some spotty biological coating.
125ROV-4	12.04.2005	04°48.6111	12°22.327	3000	Aphyric basalt crust, 4 cm thick, 3 mm glass crust with rough polyhedral joints. Interior is microcrystalline with small vesicles and 3-4 cm thick lower surfaces showing complex plastic deformation and lava stalagtites.
125ROV-6	12.04.2005	04°48.624	12°22.355	2986	Three pieces, basalt overgrown with scyphocytes, aphyric basalt, 2 mm thick glass crust, interior with large vesicles.

Station	Date	Lat. (S)	Long. (W)	Depth (m)	Rock description
125ROV-8	12.04.2005	04°48.635	12°22.345	2985	Aphyric basalt, 3 mm thick glass crust, interior is microcrystalline. Fracture surfaces normal to top of sample are coated with Fe-oxihydroxides.
125ROV-9	12.04.2005	04°48.634	12°22.355	2986	Very fresh glass from flow carapace, abundant quench fractures, <1 vol% olivine phenocrysts, max. diameter ~1mm, locally with elongate to lensoidal vesicles up to 2 x 3 cm, no small vesicles.
125ROV-10	12.04.2005	04°48.634	12°22.355	2986	Some more fragments of the same type and the same location as sample 125-9 (see above).
126CTD	12.04.2005	04°46.8	12°23.2	3063	
127CTD	13.04.2005	04°48.7	12°23.0	2959	
128CTD	13.04.2005	04°48.8	12°22.4	2967	
129CTD	13.04.2005	04°48.6	12°22.6	2982	
130ROV-1*	13.04.2005	04°48.57	12°22.417	2985	There are two types of fragments: 1. Chimney interior consisting of anhydrite and chalcopyrite. 2. Chimney crust consisting of pyrite, chalcopyrite and marcasite, partially covered by Fe-oxihydroxides.
130ROV-2*	13.04.2005	04°48.57	12°22.417	2985	Hollow chimney structure with 2 cm thick walls. Walls consist of cpy and marcasite and a 1-5 mm marcasite crust. Interior of the vent (5 x 3 x 2 cm) is extensively lined by 1-3 mm thick pyrrotine crust with beautiful blade crystals up to 1 mm in diameter.
130ROV-3*	13.04.2005	04°48.57	12°22.417	2985	Particles are 5 to <1mm, 75% pyrite particles including some collomorphic aggregates; 10% basalt glass chips (max. 5 mm); 10% anhydrite <1 mm, some larger particles are well-rounded due to resorption by seawater;<5% cpy (altered) and pyrite aggregates, <1% globugerina; rare goethite.
131GTV-1	13.04.2005	04°48.57	12°22.37	2999	Piece of aphyric basalt with 1 x 1 cm mafic xenolith. Wrinkled to bulbous crust of a sheet flow with 1 to 5 mm glassy upper surface (locally some Feox-hydrox. staining). Lower surface shows plastic deformation indicating that this is the roof of a lava lobe/tunnel. Xenoliths of gabbro (cpx to 8 mm and plag to 2 mm) up to 5 cm in diameter.
131GTV-2	13.04.2005	04°48.57	12°22.37	2999	Similar to 131-1. Crust of drained lava tube. Top surface shows ropy texture; 2 to 3 mm thick glass covered by Fe-Oxihydroxides. Margins of piece are normal fractures covered by Fe-Oxihydroxides and biology.
131GTV-3	13.04.2005	04°48.57	12°22.37	2999	Similar to 131-1 and 2. Platy slab representing the roof of a drained sheet lava flow. Top is flat and covered by <1 mm hydrothermal(?) crust. Glass is 10 mm thick and shows nice gradation over 3 mm into microcrystalline interior. Lower surface shows lava stalagtites.
131GTV-4	13.04.2005	04°48.57	12°22.37	2999	Similar to 131-1,-2, and -3. Lava tongue (4 cm thick) with 1 to 5 mm thick glass on both sides. Top surface is ropy to wrinkled.
131GTV-5	13.04.2005	04°48.57	12°22.37	2999	Aphyric lava with gabbroic xenoliths: clinopyroxene and plagioclase up to 8 mm.
132GTV-1	14.04.2005	04°48.62	12°22.34	2996	Fresh lava piece, bulbous, aphyric, 10 mm of glass on both sides.

Station	Date	Lat. (S)	Long. (W)	Depth (m)	Rock description
132GTV-2	14.04.2005	04°48.62	12°22.34	2996	Similar to 132-1, fresh surface with biological colonization.
132GTV-3	14.04.2005	04°48.62	12°22.34	2996	Similar to 132-1.
133CTD	14.04.2005	04°48.6	12°22.4	2966	
134VSR-1	14.04.2005	04°49.01	12°23.05	3000	Basaltic glass with plagioclase phenocrysts.
135VSR-1	14.04.2005	04°49.02	12°22.51	3001	Two pieces of aphyric basalt lava with 1 cm glass crust.
136VSR-1	14.04.2005	04°48.26	12°21.86	2970	Aphyric basalt glass + some globigerina.
137VSR-1	14.04.2005	04°48.23	12°21	2903	Foraminiferous sediment.
138CTD	14.04.2005	04°47.8	12°22.6	2971	
139GTV-1 to 8	14.04.2005	04°48.57	12°22.417	2985	Diverse accociation of different types of sulfides: individual cpy-rich chimneys, pyrite-marcasite-chimneys, coalesced microchimneys, anhydrite-rich pieces with varying proportions of magnetite+chalcopyrite, cavities lined with euhedral gypsyum crystals, friable magnetite-rich samples, minor sphalerite; locally oxidation => hematite bands.
140DUMMY	14.04.2005	04°48.2	12°22.9	3035	
141ROV_AC-6	15.04.2005	04°48.56	12°22.41	2985	Pyrite-marcasite crust, chalocopyrite in the interior is typically altered (pigeon color). Redbrown outer surface: Fe-oxihydroxide coating. One piece with central vug (2 x 3 cm) line with pyrrotite + isocubanite (?). Some of the fragments contain 1-3 mm layer of magnetite separating the chacopyrite and pyrite-marcasite zones.
142VSR-1	15.04.2005	04°48.75	12°22.52	3004	Several aphyric basalt glass fragments.
143VSR	16.04.2005	04°48.9	12°22.0	2983	empty
144VSR	16.04.2005	04°48.0	12°22.6	3023	empty
145CTD	16.04.2005	04°48.9	12°22.8	2974	
146ROV-1	16.04.2005	04°48.88	12°22.93	2973	Altered, highly plagioclase-phyric basalt, 20 % plagioclase phenocrysts up to 12 mm in diameter. Sample of lava crust. Glass is completely altered (clay-Mn Oxide, Fe Oxihydroxide), abundant biological colonization.
146ROV-2	16.04.2005	04°48.35	12°22.69	3024	Fresh glassy aphyric basalt; large elongate cavities: long axis (>5 cm) parallel to the flow fold axis.
146ROV-3	16.04.2005	04°47.902	12°22.618	3045	Sulfide knob on inactive chimney. Friable interior with irregular cavities lined by sphalerite and chalcopyrite (crystals <1 mm). Bulk of the piece consists of chalcopyrite-marcasite. Crust: 2 mm black Fe-oxihydrixide.
146ROV-7	16.04.2005	04°47.824	12°22.595	3048	Sphalerite-rich fragment of active smoker. Internal cavitiy (2 x 1.5 cm) lined by pyrrotite (+isocubanite?). Crust of Fe-oxihydroxide is extensively coated by white material (sulfur?) and orange-brown globules coated by Fe-oxides .
147VSR	18.04.2005	08°50.0	13°29.7	2224	empty
148VSR-1	18.04.2005	08°49	13°29.8	2230	Small chips of gray, microcrystalline aphyric basalt, trace of glass chips.
149VSR	18.04.2005	08°48.0	13°31.0	2214	empty

Station	Date	Lat. (S)	Long. (W)	Depth (m)	Rock description
150VSR-1	18.04.2005	08°48.01	13°30.3	2211	Small amount of glass particles.
151VSR-1	19.04.2005	08°47.99	13°30.1	2219	Basalt
152VSR-1	19.04.2005	08°47.99	13°29.81	2223	Several glass pieces.
153VSR-1	19.04.2005	08°47.99	13°29.29	2165	Shell fragments (sediment patch).
155ROV-1	19.04.2005	08°48.98	13°30.5	2161	Glassy basalt from talus breccia, covered by mud, rare <1mm olivine phenocrysts.
155ROV-2	19.04.2005	08°48.99	13°30.44	2172	Microcrystalline basalt, ca. 5% vesicles up to 2 mm in diamter, <1% olivine phenocrysts up to 1 mm, top coated by Mn-Oxide crust, abundant microorganisms.
155ROV-3	19.04.2005	08°49	13°30.3	2149	Four cm thick roof of lava lobe. Top surface is glassy (2 mm thick), 5 % vesicles up to 5 mm in the microcrystalline basalt below the glass crust; lower surface with stalagtite texture; rare olivine phenocrysts <1mm.
155ROV-4	19.04.2005	08°48.96	13°30.17	2195	Aphyric basalt, pillow section, microcrystalline with partially palagonitized glass crust (ca. 1 mm); 2 % vesicles up to 2 mm.
155ROV-5	19.04.2005	08°48.99	13°30.06	2199	Altered aphyric basalt with <1% pyroxene and rare plagioclase (<1 mm). Piece consists of two individual lobes showing ductile deformation.
155ROV-6	19.04.2005	08°48.99	13°30.04	2190	Piece of pillow crust with prominent striated top surface texture. Roof (3 cm thick) of partially drained pillow. Glass on both sides (top: 2 to 4 mm; base < 1mm). Partial palagonitization. 1% olivine phenocrysts up to 5 mm.
155ROV-7	19.04.2005	08°48.99	13°29.97	2221	Abundant aphyric basalt glass chips of pillow crust. Partially palagonitized.
155ROV-8	19.04.2005	08°49.04	13°29.85	2218	Single piece of microcrystalline basalt with 1% olivine phenocrysts (up to 1 mm); ca 1% vesicles (up to 2 mm). Glass crust is 1-3 mm thick and locally shows spherulitic textures.
156VSR-1	19.04.2005	08°48.43	13°30.42	2208	Basalt glass.
157VSR-1	19.04.2005	08°47.7	13°30.56	2190	Basalt glass.
158DUMMY	20.04.2005	08°53.1	13°31.2	2198	
159ROV-1	20.04.2005	08°48.18	13°30.12	2204	Glassy basalt with 1% olivine and plagioclase phenocrysts up to 1 mm, some palagonite.
159ROV-2	20.04.2005	08°48.15	13°30.12	2201	Basalt with 3 mm glass crust, <1% plagioclase phenocrysts 2% vesicles up to 2 mm, minor Fe staining.
159ROV-3	20.04.2005	08°48.06	13°30.12	2198	Aphyric glassy basalt; flow fold quenched on both sides, slight palagonitization, microcrystalline groundmass surrounds elongate cavity (long axis >4 cm parallel to fold axis).
159ROV-4	20.04.2005	08°47.99	13°30.12	2201	Aphyric glassy basalt, abundant shards <1 to 3 cm in foram./pteropod sand.
159ROV-5	20.04.2005	08°47.96	13°30.16	2186	Piece of lava protrusion, plagioclase-phyric glassy basalt, 10 vol.% plagioclase phenocrysts up to 10 mm, surface with striation marks, glass crust partially palagonitized and covered by thin layer of black Mn-oxide.

Station	Date	Lat. (S)	Long. (W)	Depth (m)	Rock description
159ROV-6	20.04.2005	08°47.81	13°30.19	2151	Abundant fragments of aphyric basalt glass shards.
159ROV-7	20.04.2005	08°47.75	13°30.21	2201	Plagioclase-phyric basalt with 2 mm glass crust, <1% plagioclase up to 1 mm, 3% vesicles up to 2 mm, several zones of shearing up to 1 cm wide oriented parallel to the surface spaced at 2-4 cm intervals. Slight Fe-Oxihydroxide staining.
159ROV-8	20.04.2005	08°47.76	13°30.21	2202	Basalt with 1-2 mm glass crust, slightly palagonitized, few plagioclase phenocrysts (< 1mm), 1 vol. % vesicles up to 1 mm.
159ROV-9	20.04.2005	08°47.5	13°30.21	2215	Pillow top is glassy (1-2 mm thick), slight palagonitization, <1% plagioclase and olivine, up to 1 mm, lower surface is ondulated, solidified lava droplets.
159ROV-10	20.04.2005	08°47.46	13°30.18	2219	Small lava fold with glassy crust (1-2 mm), plagioclase-phyric basalt, 1% plagioclase up to 1 mm.
159ROV-11	20.04.2005	08°47.46	13°30.18	2219	Lava lobe of 4 cm thickness with glassy crust on both sides, abundant palagonitization, 1% plagioclase phenocrysts up to 5 mm, rare olivine.
160VSR-1	20.04.2005	08°46.93	13°30.39	2208	Basalt glass.
161VSR-1	20.04.2005	08°46.7	13°30.57	2266	Basalt glass with plagioclase phenocrysts.
162VSR-1	21.04.2005	08°46.22	13°30.64	2273	Basalt glass with plagioclase phenocrysts.
163VSR-1	21.04.2005	08°45.43	13°30.74	2287	Basalt glass with plagioclase phenocrysts.
164CTD	21.04.2005	08°54.0	13°29.2	2122	
165VSR-1	21.04.2005	08°50	13°29.68	2225	Aphyric basalt glass.
166VSR-1	21.04.2005	08°50.51	13°29.48	2188	Chips and fragments of microcrystalline and glassy basalt.
167CTD	21.04.2005	09°00	13°29	1974	
168CTD	21.04.2005	09°00	13°28	2153	
169CTD	21.04.2005	09°00	13°27	2244	
170VSR-1	21.04.2005	09°20	13°27	2313	Sediment in vaseline with a few glass particles.
171VSR-1	21.04.2005	09°4.01	13°26.6	2320	Sediment patches.
172CTD	22.04.2005	09°7.5	13°27.0	2530	
173CTD	22.04.2005	09°7.5	13°26.0	2530	
174CTD	22.04.2005	09°7.5	13°25.0	2530	
175VSR-1	22.04.2005	09°7.5	13°25.86	2530	Olivine-phyric basalt (1% olivine phenocrysts up to 2 mm), glassy and microcrystalline fragments, moderate palagonitization.
176VSR-1	22.04.2005	09°9.02	13°25.51	2640	Basalt glass.
177CTD	22.04.2005	09°10.5	13°26.1	2654	
178CTD	22.04.2005	09°10.4	13°25.0	2582	
179CTD	22.04.2005	09°10.5	13°24.0	2284	
180CTD	22.04.2005	09°10.5	13°23.0	2372	
181VSR-1	22.04.2005	09°15.29	13°17.5	2285	Altered glass crust with sediment.
182VSR-1	22.04.2005	09°17.02	13°17.02	2072	Very few glass chips.
183VSR-1	22.04.2005	09°20.9	13°17.1	2261	empty
184VSR-1	23.04.2005	09°22.49	13°15.53	1932	Few thin rock fragments.
185CTD	23.04.2005	09°19.0	13°17.0	2370	

Station	Date	Lat. (S)	Long. (W)	Depth (m)	Rock description
186CTD	23.04.2005	09°19.0	13°16.0	1932	
187CTD	23.04.2005	09°19.0	13°15.0	2059	
188ROPV_P-1	23.04.2005	09°42.48	13°5.02	1772	Piece of aphyric basalt lava. Roof of lava lobe. Glassy crust with abundant palagonitization. Rare olivine phenocrysts (< 1 mm), ca 1% vesicles up to 5 mm. Extensive Mn-oxide coating.
188ROPV_P-3	23.04.2005	09°42.49	13°4.96	1787	Piece of aphyric lava lobe. 1 to 2 mm glassy crust with intense palagonitization. Ca. 5 % tubular vesicles (1 mm x 10 mm) concentrated below crust. Extensive Mn-oxide coating and biological colonization.
188ROPV_P-4	23.04.2005	09°42.49	13°4.8	1857	Piece of aphyric basalt lava lobe with rare olivine phenocrysts. Glass crust (1 to 3 mm) is heavily palagonitized. Some Fe-oxihydroxide alteration and abundant worm tubes. Vesicles: <1%, < 1mm.
188ROPV_P-5	23.04.2005	09°42.39	13°4.67	1864	Two pieces of small lava lobe. Glass crust (1 to 2 mm) is strongly palagonitized. Vesicles: < 1%, < 1 mm.
188ROPV_P-7	23.04.2005	09°42.36	13°4.51	1882	Aphyric basalt pillow. Glass crust (1 to 2 mm) is strongly palagonitized. Coated by Mn-oxide and some biological colonization.
189CTD	23.04.2005	09°27.0	13°14.0	1701	
190CTD	23.04.2005	09°27.0	13°16.0	2083	
191CTD	23.04.2005	09°27.0	13°12.0	1886	
192CTD	24.04.2005	09°30.0	13°13.0	1653	
193CTD	24.04.2005	09°32.5	13°12.9	1458	
194ROPV_P-1	24.04.2005	09°34.37	13°12.95	1454	One piece of aphyric pillow basalt. Vesicles: 3% up to 3 mm. Palagonitized glass crust (1-3 mm); Mn-oxide and Fe-oxihydroxide coating and some biology.
194ROPV_P-4	24.04.2005	09°34.37	13°12.86	1429	Section of aphyric pillow basalt. Vesicles: 5% up to 10 mm. Palagonitized glass crust. Extensive Mn-oxide coating. Biological colonization including trunk of gorgonaria.
194ROPV_P-6	24.04.2005	09°34.37	13°12.77	1436	Aphyric basalt. Extensive palagoniti.zation and Mn-oxide coating.
194ROPV_P-7	24.04.2005	09°34.37	13°12.67	1448	Roof of lava lobe; Top: wrinkled glass (ca. 5 cm), fresh. Aphyric. Vesicles: 3%, up to 1 mm.
194ROPV_P-8	24.04.2005	09°34.41	13°14.53	1465	Section of pillow. Rare olivine phenocrysts (up to 1 mm). Vesicular central part (30% up to 20 mm, locally coalesced). Tubular vesicles (up to 4 cm long) oriented normal to the exterior in the outer 10 cm of the section. Outermost 1-2 cm are vesicle-free. Some glassy patches preserved.
194ROPV_P-9	24.04.2005	09°34.43	13°12.52	1465	Three pieces of aphyric basalt with 1 to 3 mm glass crust.
194ROPV_P-10	24.04.2005	09°34.37	13°12.5	1470	Vesicular aphyric basalt. Vesicles: 10%, up to 5 mm, locally coalesced. Outer zone (1 cm) is vesicle-free. Glass crust (1-2 mm) is slightly palagonititzed.

Station	Date	Lat. (S)	Long. (W)	Depth (m)	Rock description
194ROPV_P-11	24.04.2005	09°34.38	13°12.49	1470	Piece of aphyric lava fold with 1 mm glass crust on both sides. Central zone contains 20% vesicles up to 1 cm; abundant tubular vesicles oriented normal to the exterior. Outer 1 cm on both sides are vesicles-free.
194ROPV_P-12	24.04.2005	09°34.38	13°12.34	1460	Crust of aphyric lava lobe with wrinkely lower surface. Slightly palagonitized glass crust (1 to 2 mm). Vesicles are tubular, oriented normal to the surface (20%).
194ROPV_P-13	24.04.2005	09°34.38	13°12.34	1468	Slab of aphyric sheet flow exposed in collapse pit. Roof of lava tunnel. Top surface is wrinkled on 10 cm scale. Fresh glassy crust with prominent perlite texture. Lower surface with abundant lava droplets, thin-walled bubbles and linear lava stalagtites.
195CTD	24.04.2005	09°34.5	13°12.5	1402	
196CTD	24.04.2005	09°31.5	13°13.0	1550	
197CTD	25.04.2005	09°33.9	13°12.7	1477	
199CTD	25.04.2005	09°33.0	13°12.9	1473	
200ROV_P-1	25.04.2005	09°32.99	13°12.92	1469	Aphyric pillow basalt. Vesicles: 5% up to 10 mm. Extensive Mn-Oxide coating. Patch of glassy crust, partially palagonitized.
200ROV_P-2	25.04.2005	09°32.96	13°12.80	1523	Pillow basalt. Olivine phenocrysts: <1% up to 1 mm. Vesicles: 5%, irregular shapes, up to 10 mm. Extensive Mn-oxide coating, 1 mm palagonitized glass crust.
200ROV_P-3	25.04.2005	09°32.90	13°12.72	1505	Piece of lava lobe roof. Aphyric. Top surface shows mm-scale scretch marks (parallel to flow direction) and cm-scale flow folds (long axis normal to flow direction). Fresh glass crust (3 mm). Vesicles: 10% round and tubular. Lower surface: irregular stalagtite texture.
200ROV_P-5	25.04.2005	09°32.93	13°12.51	1494	Bright orange Fe-oxihydroxide mud and few small pieces of semi-lithified material.
200ROV_P-6	25.04.2005	09°32.92	13°12.53	1496	Piece of 6 cm thick aphyric lava crust. Glass crust (1-2 mm) with minor Mn-oxide coating. Upper layer is vesicle-free; lower 3 cm contain 20% tubular vesicles (up to 3 cm long and 0.5 cm wide) normal to surface with regular spacing.
200ROV_P-7	25.04.2005	09°32.88	13°12.55	1495	Semi-lithified pieces of Fe-oxihydroxides; crude layering, no apparent Mn-oxides.
200ROV_P-12	25.04.2005	09°32.71	13°12.55	1495	Section of aphyric pillow basalt. Vesicles: 10% round to irregular, locally coalesced (up to 2 cm). Glass crust (2 mm) with Mn-oxide coating and biological colonization.
201VSR-1	25.04.2005	09°31.98	13°12.21	1551	Pelagic sediment.
202VSR-1	25.04.2005	09°32.49	13°12.71	1512	Basalt glass.
203VSR-1	26.04.2005	09°32.72	13°12.65	1509	Basalt glass.
204VSR-1	26.04.2005	09°33.01	13°12.36	1518	Basalt glass.
205VSR-1	26.04.2005	09°33.5	13°12.53	1497	One pillow fragment with glass crust and several glass chips.
206CTD	26.04.2005	09°33.3	13°12.5	1469	
207ROV	26.04.2005	09°32.9	13°12.5	1510	

Station	Date	Lat. (S)	Long. (W)	Depth (m)	Rock description
208CTD	26.04.2005	09°32.8	13°12.6	1501	
209GTV-1	26.04.2005	09°32.86	13°12.52	1511	Glassy volcanic crust; partially altered.
209GTV-2	26.04.2005	09°32.86	13°12.52	1511	Orange to brown semi-lithified Fe-oxihydroxides; numerous pieces of fragile crusts up to 15 x 10 x 1 cm; fine grained.
210VSR-1	26.04.2005	09°33.83	13°12.50	1482	Several pieces of aphyric basalt, abundant glass shards.
211VSR-1	26.04.2005	09°34.13	13°12.55	1488	Fresh aphyric basalt glass.
212VSR-1	26.04.2005	09°34.55	13°12.40	1413	Some glass chips.
213GTV-1	27.04.2005	09°32.83	13°12.55	1513	Basalt glass chips.
213GTV-2	27.04.2005	09°32.83	13°12.55	1513	Fe-oxihydroxide crusts.
213GTV-3	27.04.2005	09°32.83	13°12.55	1513	Thin (<1 mm) sheets of sulfides.
214GTV-1	27.04.2005	09°32.84	13°12.54	1511	Fresh aphyric basaltic glass chips.
214GTV-2	27.04.2005	09°32.84	13°12.54	1511	Fe-oxihydroxide crusts.
214GTV-3	27.04.2005	09°32.84	13°12.54	1511	Thin sheets (<1 mm) of sulfides.
215OFOS	27.04.2005	09°32.1	13°12.9	1550	
216CTD	27.04.2005	09°32.8	13°12.9	1509	

*: Sample position accurate within +/- 1 to 2 m relative to the beacon set at 4°48,559'S; 12° 22,413'W
Abbreviations for sampling equipment
GTV: TV grab samples
ROV_AC: Accidentially sampled material during ROV dive due to seafloor contact
ROV_P: Sample taken on position with ROV manipulators
VSR: Vulkanit Stossrohr (wax-corer for volcanic rocks)
ROV-PC: Particle Catcher deployed by ROV

1.7. Concluding Remarks

Cruise M64/1 was a very successful cruise without any major technological or logistical problems. The cooperation between the crew and the scientists resulted in a large number of successful sampling stations and numerous excellent geologic and biologic samples. Several outstanding results have been obtained like the sampling of the hottest vents known from the Mid-Atlantic Ridge, the finding of the southernmost vent field on the Mid-Atlantic Ridge, and the definition of several new targets for further exloration in this area. Consequently, M64/1 has made important new contribution to our understanding of the volcanic, hydrothermal and biologic processes on a slow-spreading axis and it also paved the way for further cruises during the lifetime of SPP 1144.

1.8. References

Baker, E.T. and Milburn, H.B., 1997. MAPR: a new instrument for hydrothermal plume mapping. RIDGE events, 8: 23-25.

Baker, E.T., Tennant, D.A., Feely, R.A., Lebon, G.T. and Walker, S.L., 2001. Field and laboratory studies on the effect of particle size and composition on optical backscattering measurements in hydrothermal plumes. Deep-Sea Research. Part I: Oceanographic Research Papers, 48(2): 593-604.

Charlou, J.L., Donval, J.P., Fouquet, Y., Jean-Baptiste, P., and Holm, N. (2002). Geochemistry of high H_2 and CH_4 vent fluids issuing from ultramafic rocks at the Rainbow hydrothermal field (36°14'N, MAR). Chem. Geol. 191, 345-359.

Desbruyères, D., Biscoito,M, Caprais, J.-C., Colaco, A., Comtet, T., Crassous, P., Fouquet, Y., Khripounoff, N., Le Bris, N., Olu, K., Riso, R., Sarradin, P.-M., Segonzac, M. and Vangriesheim, A. (2001): Variations in deep-sea hydrothermal vent communities an the Mid-Atlantc Ridge near the Azores plateau. – Deep-Sea Research I 48: 1325-1346.

Grasshoff, K., Kremling, K., Ehrhardt, M., 1999. Methods of Seawater Analysis. 3rd edition, 600 p., Wiley-VCH.

Kadko, D. C., Rosenberg, N. D., Lupton, J. E., Collier, R. W., and Lilley, M. D. (1990). Chemical reaction rates and entrainment within the Endeavour Ridge hydrothermal plume. Earth Planet. Sci. Lett. 99, 315-335.

Localli, C., Torsi, G., 2001. Voltammetric trace metal determinations by cathodic and anodic stripping voltammetry in environmental matrices in the presence of mutual interference. Journal of Electroanalytical Chemistry 509, 80-89.

Obata, H., van den Berg, C.M.G., 2001. Determination of picomolar levels of iron in seawater using catalytic stripping voltammetry. Analytical Chemistry 73, 2522- 2528.

Shank, T. (2004): The evolutionary puzzle of seafloor life. - Oceanus Magazine • Vol. 42, No.2 http://oceanusmag.whoi.edu/v42n2/shank.html.

van Damm, K.L., 2004. Evolution of the hydrothermal system at the East Pacific Rise 9°50'N: geochemical evidence for changes in the upper oceanic crust. In: Mid-Ocean Ridges: Hydrothermal Interactions between the Lithosphere and Oceans.

Seifert, R., Delling, N., Richnow, H.H., Kempe, S., Hefter, J., and Michaelis, W. (1999). Ethylene and methane in the upper water column of the subtropical Atlantic. Biogeochemistry 44, 73-91.